

MAHATMA GANDHI UNIVERSITY
PROJECT REPORT

EFFECTS OF SOLAR WIND TRANSIENTS
ON OUR EARTH

Year: 2020-2022

**In partial fulfilment of the requirement of the award of
Master of Science Degree in Physics**

By

JESNA P B

M.Sc. PHYSICS

REG NO. AM20PHY007

Under the supervision of

Dr. PRIYA PARVATHI AMEENA JOSE

Department of Physics

St. Teresa's College, Ernakulam

and

Dr. K P ARUN BABU

Department of Physics

St. Albert's College, Ernakulam



**ST. TERESA'S COLLEGE (AUTONOMOUS),
ERNAKULAM, KOCHI-682011**

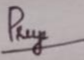
DEPARTMENT OF PHYSICS AND CENTRE FOR RESEARCH
ST. TERESA'S COLLEGE (AUTONOMOUS), ERNAKULAM

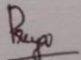


M.Sc. PHYSICS PROJECT REPORT

Name : JESNA P B
Register Number : AM20PHY007
Year of Work : 2020-2022

This is to certify that the project "EFFECTS OF SOLAR WIND
TRANSIENTS ON OUR EARTH" is the work done by **Jesna P B**

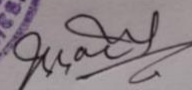

Dr. Priya Parvathi Ameena Jose
Staff Member in charge


Dr. Priya Parvathi Ameena Jose
Head of the Department

Submitted for the university examination held in St. Teresa's College,
Ernakulam.

Examiners

1. Dr. Issac Paul
2. Dr. Gishamo Mathew




Date: 13.06.2022

ST. TERESA'S COLLEGE (AUTONOMOUS),
ERNAKULAM



CERTIFICATE

This is to certify that the project entitled “EFFECTS OF SOLAR WIND TRANSIENTS ON OUR EARTH” is a bonafied work carried out by **JESNA P B**, in partial fulfilment of the requirements for the award of the degree of Master of Science in Physics during the academic year 2020-2022 and has not been included in any other works submitted previously for the award of any degree.

Dr. PRIYA PARVATHI AMEENA JOSE
Assistant Professor
Department of Physics
St. Teresa's College (Autonomous),
Ernakulam

Place: Ernakulam

Date: 10 June 2022





ST. ALBERT'S COLLEGE (AUTONOMOUS)
ERNAKULAM - 682018
Affiliated to Mahatma Gandhi University, Kottayam

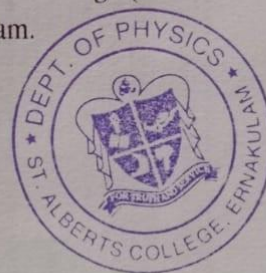
DEPARTMENT OF PHYSICS
Email: physics@alberts.edu.in
Website: www.alberts.edu.in/department-of-physics

CERTIFICATE

This is to certify that the work incorporated in the thesis entitled "EFFECTS OF SOLAR WIND TRANSIENTS ON OUR EARTH", submitted by 'JESNA P B', towards the partial fulfilment of the requirements for the award of the degree, Master of Science in Physics is a bonafied record of the work carried out by the candidate, under my supervision. The work presented here or any part of it has not been included in any other thesis submitted previously for the award of any degree or diploma from any other University or institution.

Dr. Arun Babu K P
Asst. Professor,
Dept. Of Physics,
St. Albert's College (Autonomous)
Ernakulam.

Place : Ernakulam
Date : 9 June 2022.



DECLARATION

I, JESNA P.B., hereby declare that the project report entitled “**EFFECTS OF SOLAR WIND TRANSIENTS ON OUR EARTH**” is an authentic record of the work carried out by me under the guidance of **Dr. K P ARUN BABU**, Assistant Professor, Department of Physics, St. Albert’s College, Ernakulam, and **Dr. PRIYA PARVATHI AMEENA JOSE**, Assistant Professor, Department of Physics, St. Teresa’s College, Ernakulam.

The data and conclusions drawn are based on the calculations done by myself. This is my original work and the report submitted has not been duplicated from any other source.

JESNA P B
AM20PHY007

Date: 10 June 2022

Place: Ernakulam

AKNOWLEDGEMENT

First of all, I would like to thank the Almighty God for being able to complete this project with success.

I take this opportunity to express my profound gratitude and deep regards to my guide **Dr. K P Arun Babu**, Assistant Professor, St. Albert's College, Ernakulam, and **Dr. Priya Parvathi Ameena Jose**, Assistant Professor, St. Teresa's College, Ernakulam, for their exemplary guidance, monitoring, support and constant encouragement without which this project would not be able to exist in the present shape. The blessings, help and guidance given by them time to time shall carry us a long way in the journey of life on which we are about to embark. They have taken pain to go through the project and make necessary corrections as when needed. I am extremely thankful to all other faculties of the department of physics, for their constant support.

I would like to express my thanks to all respondents and colleagues in developing the project. I'm grateful to my parents for their blessings and constant encouragement throughout the project.

ABSTRACT

Our Earth is experiencing a continuous stream of charged particles released from the upper atmosphere of the Sun known as the solar wind. The dynamic pressure and magnetic field of solar wind are compressing the magnetosphere in the day-side to bow-shock-nose. During a solar transient event, an enhancement in the solar wind parameter such as density, magnetic field, and flow speed was observed, causing a significant change in our magnetosphere, also known as geomagnetic storms. In this work we are analysing the relationship of the ram pressure and magnetic field of solar transient events to the geomagnetic storms. We are analysing the solar transient events during the period from 2001 to 2020 with a four year gap.

CONTENT

1. INTRODUCTION	2
1.1 Sun	2
1.1.1. Solar interior.....	3
1.1.2. Solar atmosphere	4
1.1.3. Corona	5
1.2 Solar cycle.....	7
1.3 Solar wind	9
1.4 Coronal Mass Ejection	11
1.5 Geomagnetic storms.....	14
1.6 Sun-Earth connections	16
2. DATA ANALYSIS AND INTERPRETATION	18
2.1 Solar wind parameters	19
2.2 Variation of flow pressure and magnetic field with DST.....	21
2.3 Dependency of dynamic pressure and magnetic field on SymH.....	22
2.4 Data analysis by integration	24
2.5 Observations.....	37
3. CONCLUSION	39
4. FUTURE WORKS	43
5. BIBLOGRAPHY	44

1. INTRODUCTION

Our Earth is experiencing a continuous stream of charged particles released from the upper atmosphere of the Sun known as the solar wind. The dynamic pressure and magnetic field of solar wind are compressing the magnetosphere in the day-side to bow-shock-nose. During a solar-transient event the solar wind cause a significant change in our magnetosphere known as geomagnetic storms.

We are analysing the solar transient events during the period from 2001 to 2020 with a four year gap.

1.1. SUN

The Sun is the star at the centre of the Solar System. It is nearly perfect ball of hot plasma heated to incandescence by nuclear fusion reactions in its core, radiating the energy mainly as visible light, ultraviolet light, and infrared radiation. The sun was born from a giant molecular cloud which began to gravitationally collapse and fragment. This process of collapse and fragment continued until one of these fragments attained a central temperature large enough to start hydrogen fusion. It is the most important source of energy for life on Earth. Currently the Sun is in a stable configuration, where it is hydrostatic equilibrium ($\nabla P = -\rho g$). The sun will continue to maintain in this stable state for about 100 times its current size and begin to shedding its outer layer due to successive nuclear burning and resulting total loss of outer layer, in which all nuclear burning has stopped, called a white dwarf. According to spectral class, the Sun is a main sequence star of spectral type G2V. The Sun has a total luminosity, $L = (3.84 \pm 0.04) \times 10^{26}$ W, Mass, $M = (1.9889 \pm 0.0003) \times 10^{30}$ kg and Radius, $R = (6.959 \pm 0.007) \times 10^8$ m.

1.1.1. SOLAR INTERIOR

This is usually divided into three main regions: the sun's interior, the solar atmosphere, and the visible surface which lies between the interior and the atmosphere.

There are three main parts to solar interior: the core, the radiative zone and the convective zone. The core is at the centre. It is the hottest region, where the nuclear fusion that power the sun occur. The temperature in the core is about 1.5×10^7 K and the pressure exceeds 2.5×10^{11} atm and extends up to $0.25R_{\odot}$. Moving outward, next comes the radiative zone ($0.25-0.70R_{\odot}$). Its name derived from the way energy is carried by photons as thermal radiation. The temperature drops from about 7×10^6 K at bottom of the radiative zone to 2×10^6 K just below the convective zone. Due to high densities in the radiative zone the mean free path of photons is very small. Hence it can take tens to hundreds of thousands of years for photon to escape. The third and final region of solar interior is the convective zone ($0.7-1.0R_{\odot}$). It is also named after the dominant mode of energy flow in this layer, heat move upward via rolling convection. The temperature of convective zone is lower than that of radiative zone and heavier atoms are not fully ionized. As a result, radiative heat transport is less effective. Thermal convection carries the majority of the heat outward to the Sun's photosphere, the boundary between sun's interior and the solar atmosphere. It is what we see as the visible "surface" of the Sun. The material cools off at the photosphere, which increases its density and causes it to sink to the base of the convection zone. Above the photosphere visible sunlight is free to propagate into space, and its energy escapes the Sun entirely.

The thin interface between radiative zone and convective zone is known as

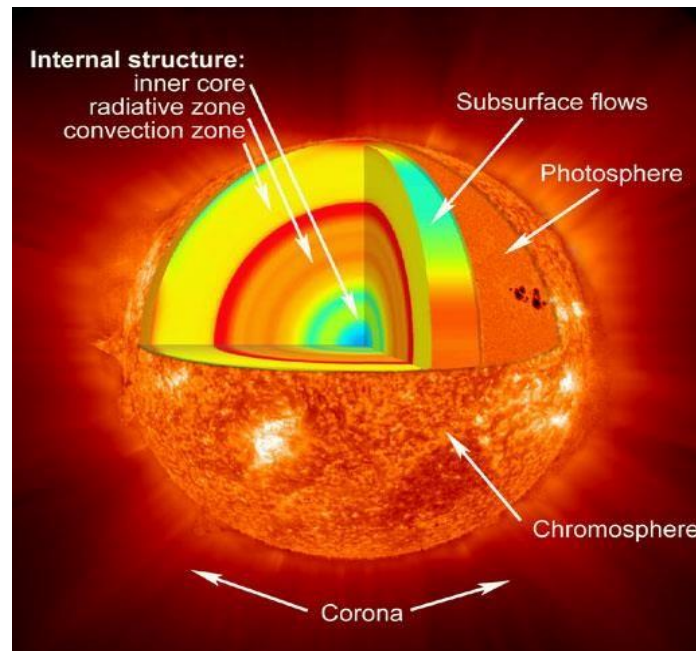


Fig1: shows the different layers of Sun. At the centre is the corona where fusion takes place. The energy generated at corona is transmitted to radiative zone where solar plasma is cool enough to form ionized atoms and becomes optically thick. Hence it is convectively unstable and energy is transported through mass motion in convection zone. (Image courtesy: Geyser land observatory)

tachocline. The fluid motions found in the convection zone slowly disappear from the top of this layer to its bottom where the conditions match those of the calm radiative zone. It is believed that the Sun's magnetic field is generated by a magnetic dynamo in this layer. The changes in fluid velocities across the layer (shear flow) can stretch magnetic field lines of force and make them stronger. This change in flow velocity gives this layer its alternative name-the tachocline. There also appears to be sudden change in chemical composition across this layer.

1.1.2. SOLAR ATMOSPHERE

The atmosphere of the Sun comprises chromosphere, solar transition region, corona, and heliosphere. The solar atmosphere is an inhomogeneous mix of different plasma properties due to up-flows, down-flows, heating, cooling and other dynamic process. The temperature decreases in the photosphere, reaching a minimum in the chromosphere, then slowly rises until there is a

rapid increase at the transition region which continues into the corona. This rapid increase in temperature is called ' coronal heating problem'. [1]

1.1.3. CORONA

The corona is the outer atmosphere of the Sun. It extends many thousands of kilometres above the visible surface of the Sun, gradually transforming into the solar wind that flows outward through our Solar System.

The material in the corona is an extremely hot but very tenuous plasma. The temperature in the corona is more than a million degrees, much hotter than the temperature at the Sun's surface which is around 5,500°C. The pressure and density in the corona are much, much lower than in Earth's atmosphere.

The corona is above the Sun's lower atmosphere, which is called the chromosphere. A relatively narrow area called the transition region, from thousands of degrees in the chromosphere to more than a million degrees in the corona. The density of plasma falls rapidly through the transition region moving upward from the chromosphere to corona.

We normally cannot see the solar atmosphere, including the corona. The surface of the Sun is far too bright to allow a glimpse of the much fainter corona. During a total solar eclipse, the corona briefly comes into view as the Moon blocks out the solar surface. A special instrument called coronagraph allows astronomers to view the corona at other times. Some coronagraphs are used with ground-based telescope, others are carried on satellites. [4]

The electron density of the solar corona ranges from $\sim 10^{14} \text{ m}^{-3}$ at its base, 2500 km above the photosphere. The temperature in corona is generally above $1 \times 10^6 \text{ K}$. The high temperature reached in the corona gives rise to

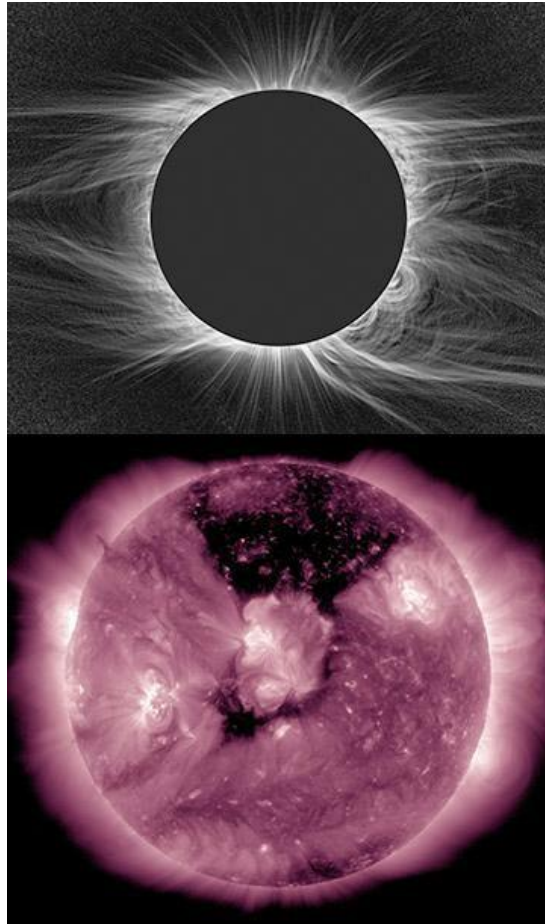


Fig 2: Two views of corona: during an eclipse (top) and ultraviolet light (bottom)

(Credit: NASA)

extreme ultraviolet (EUV) and X-ray emission, which have highly ionized ion lines as a prominent feature. The visible corona during eclipse is due to Thomson scattering of photospheric light from free electrons in the coronal plasma. The corona has a number of components:

1. K-corona (kontinuierliches) is composed of Thompson-scattered photospheric radiation and dominates below $\sim 2R_{\odot}$. As a result of the Thompson scattering mechanism, the scattered light is strongly polarized parallel to the solar limb. The high temperatures mean the electrons have high thermal velocities. This will wash out the Fraunhofer lines, producing a white-light continuum. The intensity of the K-corona is proportional to the density summed along the line-of-sight.

2. F-corona (Fraunhofer) is composed of Rayleigh-scattered photospheric radiation by dust particles and dominates above $\sim 2R_{\odot}$. It forms a continuous spectrum with superimposed Fraunhofer absorption lines. The radiation has a very low degree of polarization. The F-corona is also known as Zodiacal light, it can be seen with the naked eye at dawn or dusk under favourable conditions.
3. E-corona (Emission) is composed of line emission from visible to EUV due to various atoms and ions in the corona. It contains many forbidden line transitions; thus, it contains many polarization states.
4. T-corona (Thermal) is composed of thermal radiation from heated dust particles. It is a continuous spectrum according to the temperature and colour of the dust particles. [1]

1.2. SOLAR CYCLE

Our sun is a huge ball of electrically-charged hot gas. This charged gas moves, generating a powerful magnetic field. The sun's magnetic field goes through a cycle, called the solar cycle. Every 11 years, the sun's magnetic field completely flips. This means that the sun's north and south poles switch places. Then it takes about another 11 years for the sun's north and south poles to flip back again. The 11-year cycle in which the sun's magnetic field goes through result in formation of sunspots. As the magnetic field changes, so does the amount of activity on the sun's surface. The point of highest solar activity during a cycle is known as solar maximum and point of lowest solar activity is solar minimum. [6]

One way to track the solar cycle is by counting the number of sunspots. The beginning of a solar cycle is a solar minimum or when the sun has the least sunspots. Overtime, the solar activity and the number of sunspots increases. The middle of the solar cycle is the solar maximum or when the sun has the most sunspots. As the cycle ends, it fades back to the solar minimum and a

new cycle begins. Giant eruptions on the sun, such as solar flares and coronal mass ejections, also increases during the solar cycle. [6]

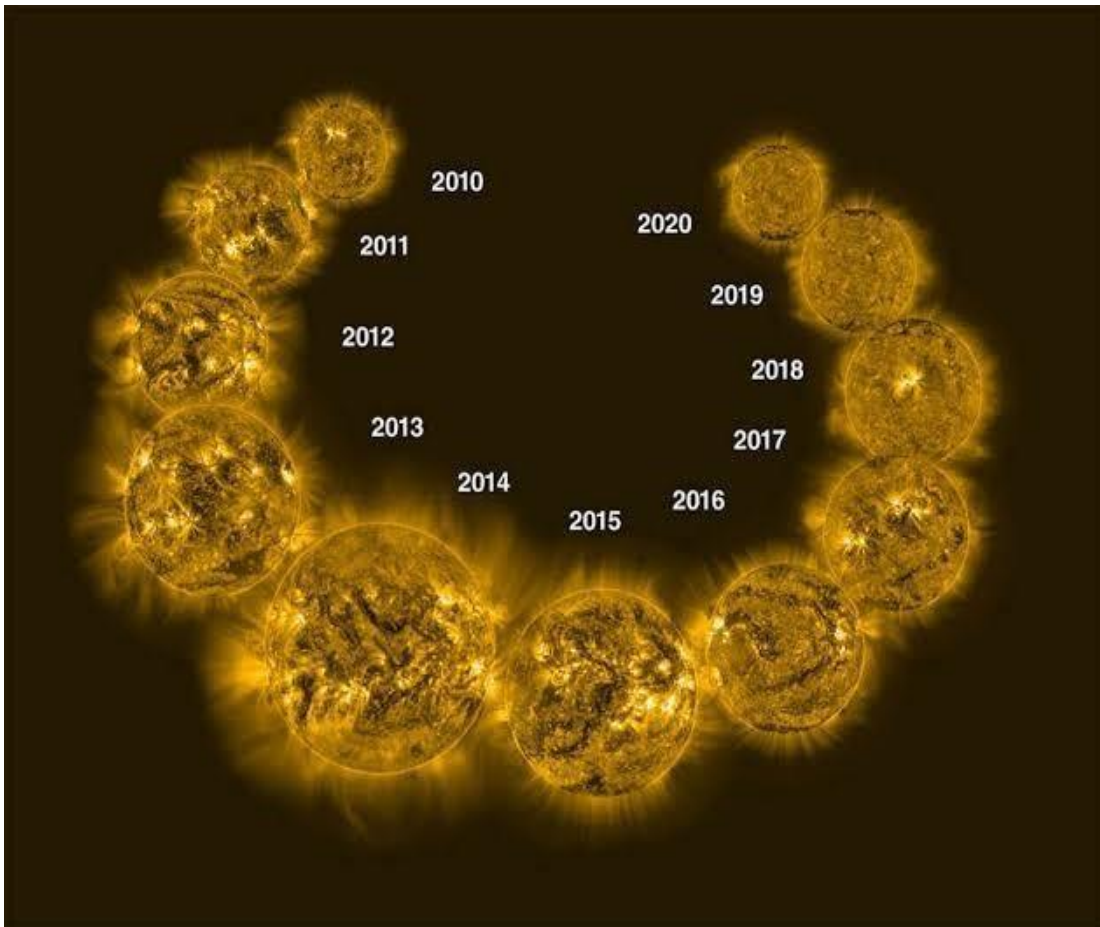


Fig 3: Evolution of the Sun in extreme ultraviolet light from 2010 through 2020, as seen from the telescope aboard Europe's PROBA2 spacecraft. (Credit: Dan Seaton/European Space Agency (Collage by NOAA/JPL-Caltech))

The 11-year-old cycles are numbered sequentially starting with observations made in 1750s. Ellery Hale first linked magnetic fields and sunspots in 1908. Although sunspots were known as early as 1600, no one noticed that their number changed with time until the German amateur astronomer Samuel Heinrich Schwabe announced the 11-year cycle in 1843. It was 15 years later that an English amateur astronomer, Richard Christopher Carrington, recognised the latitude drift of the sunspots. The most important result of Carrington's observations was the establishment of a zone leap: after both sunspot belts during one 11-year cycle have approached the equator from

north and south, just at the beginning of the next cycle, the zone leap takes place. While the last few spots of the old cycle dissolve close to the equator, new spots start to appear at high latitudes in two belts north and south of the equator from about 25° and 35° . These belts then drift towards the equator as did the belts of the old cycle. Swiss astronomer Rudolf Wolf studied historical sunspot records and proposed the scheme still used for numbering solar cycles, with solar cycle 1 beginning in 1755, the earliest year for which he found reliable sunspot numbers. The 22-year magnetic cycle was discovered in 1925 by the American astronomer George Ellery Hale. [8]

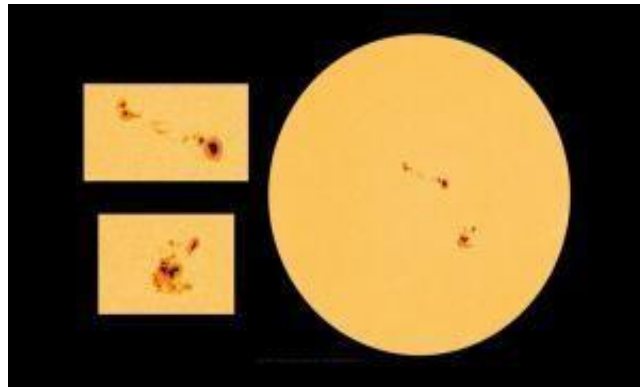


Fig 4: Sunspots

1.3. SOLAR WIND

One of the most remarkable discoveries about the Sun's atmosphere is that it produces a stream of charged particles (protons and electrons) that we call the solar wind. These particles flow outward from the sun into the solar system with a speed of about 400 km per second. The solar wind exists because the gasses in the corona are so hot and moving so rapidly that they cannot be held back by solar gravity.

Although the solar wind materials are very, very rarefied, the sun has an enormous surface area. Astronomers estimate that the sun is losing about 10 million tons of materials each year through this wind. In visible photographs, the solar corona appears fairly uniform and smooth. X-ray

and EUV pictures show that the corona has loops, plumes and both bright and dark regions. Large dark regions of corona that are relatively cool and quiet are called coronal holes. In these regions, magnetic field lines stretch far out into space away from the sun, rather than looping back to the surface. The solar wind comes predominantly from coronal holes, where gas can stream away from the sun into space unhindered by magnetic fields. Hot coronal gas, on the other hand, is present mainly where magnetic fields have trapped and concentrated it.

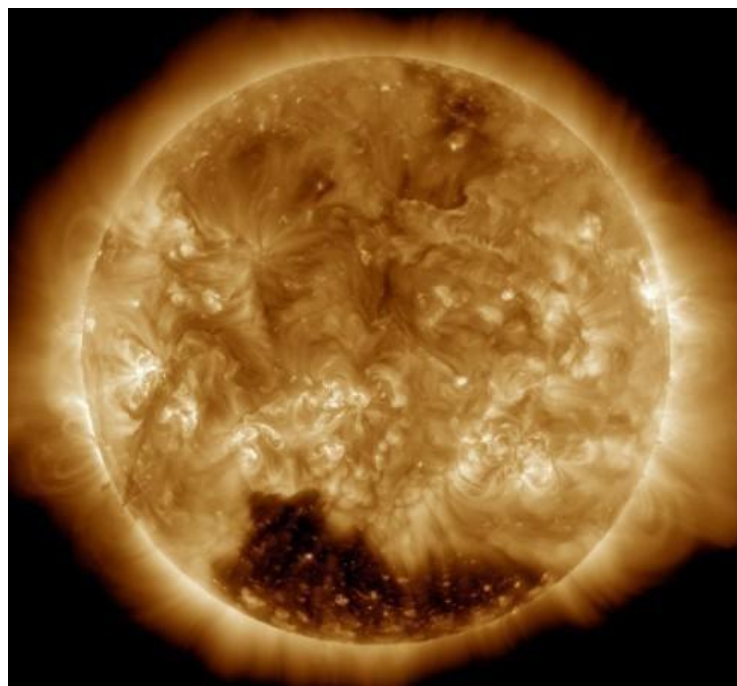


Fig 5: Coronal hole: the dark area visible near the Sun's South pole on this Solar Dynamics Observer spacecraft image is a coronal hole (credit: modification of work by NASA/ SDO)

At the surface of the Earth, we are protected to some degree from the solar wind by our atmosphere and earth's magnetic field. However, the magnetic field lines come into earth at the north and south magnetic poles. Here, charged particles accelerated by the solar wind can follow the field down into our atmosphere. As the particles strike molecules of air, they cause them to glow, producing beautiful curtains of light called the auroras or the northern and southern lights.[7]



Fig 6: Aurora: the colourful glow in the sky results from charged particles in solar wind interacting with Earth's magnetic fields. The stunning display captured here occurred over Jokularison lake in Iceland in 2013 (credit: Moyan Brenn)

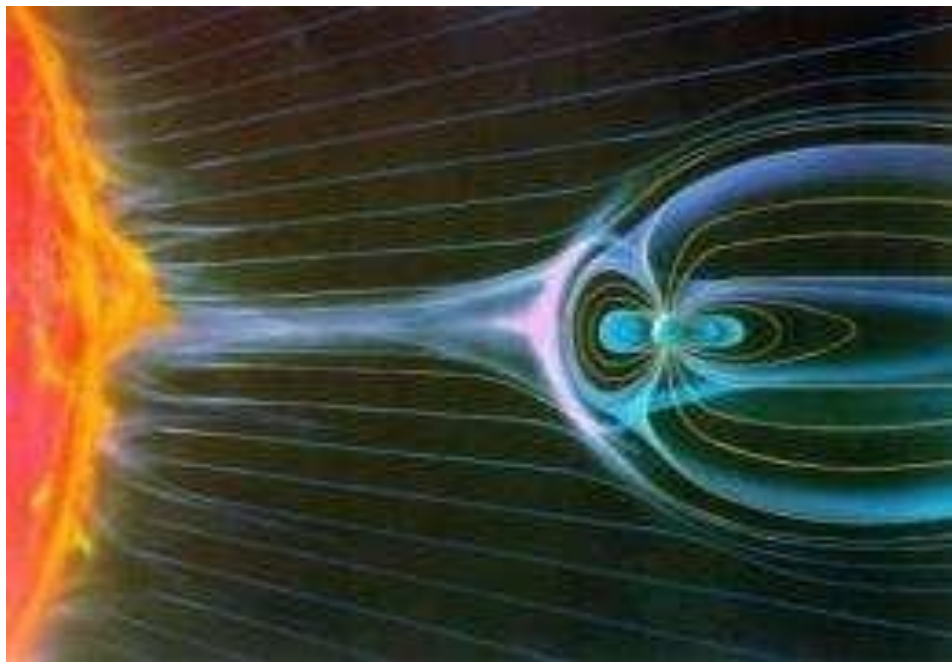


Fig 7: An artistic view of solar wind and Earth's magnetosphere. It shows how the solar wind rearranges the Earth's magnetosphere. It is compressing the magnetic field in the side facing sun and elongates same in other end (credit: NASA)

1.4. CORONAL MASS EJECTION (CME)

CMEs are large expulsion of plasma and magnetic field from the sun's corona. They can eject billions of tons of coronal material and carry an

embedded magnetic field (frozen in flux) that is stronger than the background solar wind interplanetary magnetic field (IMF) strength. CMEs travel outward from the Sun at a speed ranging from lower than 250 km/s to as fast as near 3000 km/s. The fastest Earth directed CMEs can reach our planet in as little as 15-18 hours. Slower CMEs can take several days to arrive. They expand in size as they propagate away from the Sun and larger CMEs can reach a size nearly a quarter of the space between Earth and Sun by the time it reaches our planet.

The more explosive CMEs generally begin when highly twisted magnetic field structure contained in the Sun's lower corona become too stressed and realign into a less tense configuration - a process called magnetic reconnection. This can result in the sudden release of electromagnetic energy in the form of a solar flare: which typically accompanies the explosive acceleration of plasma away from the Sun - the CME. These types of CMEs usually take place from areas of the Sun with localized fields of strong and stressed magnetic flux: such as active region associated with sunspot groups. CMEs can also occur from location where relatively cool and denser plasma is trapped and suspended by magnetic flux extending up to the inner corona - filaments and prominences. When these flux ropes reconfigure, the denser filament or prominence can collapse back to the Solar surface and be quietly reabsorbed, or CME may result. CMEs traveling faster than the background solar wind speed can generate a shock wave. These shock waves can accelerate charged particles ahead of them; causing increased radiation storm potential or intensity.

Important CME parameters used in analysis are size, speed and direction. These properties are inferred from orbital satellite's coronagraph imagery by Space Weather Prediction Center (SWPC) forecast to determine any Earth-impact likelihood. The NASA Solar and Heliospheric Observatory (SOHO)

carries a coronagraph known as the Large Angle and Spectrometric Coronagraph (LASO). This instrument has two ranges for optical imaging of the Sun's corona: C2(covers distance range of 1.5 to 6 solar radii) and C3(range of 3 to 32 solar radii). The LASO instrument is currently the primary means used by forecasters to analyse and categorize CMEs; However, another coronagraph is on the NASA STEREO-A spacecraft as an additional source.

Imminent CME arrival is first observed by the Deep Space Climate Observatory (DSCOVR) satellite, located at the L1 orbital area. Sudden increases in density, total IMF strength, and solar wind speed at the DSCOVR spacecraft indicate arrival of CME associated interplanetary shock ahead of magnetic cloud.

Important aspects of an arriving CME and its likelihood for causing more intense geomagnetic storming include the strength and direction of IMF beginning with shock arrival, followed by arrival and passage of the plasma cloud and frozen in flux magnetic field. More intense level of geomagnetic storming is favoured when the CME enhanced IMF becomes more pronounced and prolonged in south direct orientation. Some CMEs show predominantly one direction of magnetic field during its passage, while most exhibit changing field directions as the CME passes over earth. Generally, CMEs that impact earth's magnetosphere will at some point have an IMF orientation that favours generation of geomagnetic storming.[2]

In coronagraphic images, a CME can be recognised as bright features moving to progressively larger heliocentric distances. The CME occupies a portion of the coronal images indicating a finite angular extent and hence defines a finite quantity of matter expelled from the sun. CMEs are ejected into the ambient medium, which expands as solar wind. The CMEs and the

solar wind are exchange momentum. If a CME moves faster than the characteristics speed of the ambient medium it can drive a shock which have additional consequences. [10]

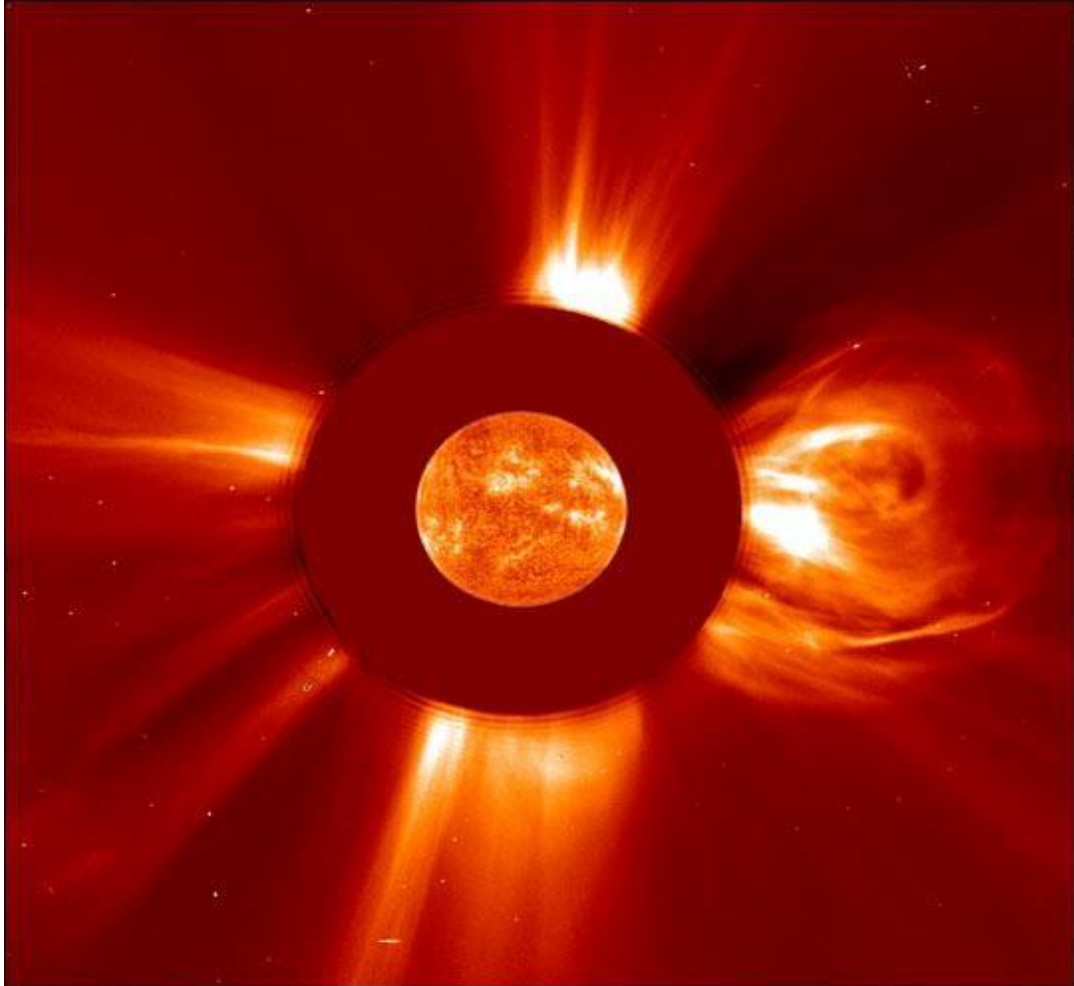


Fig 8: An image of a coronal mass ejection observed by NASA's Solar and Heliospheric Observatory, or SOHO, satellite in 2001.(Credit: ESA/NASA/SOHO)

1.5. GEOMAGNETIC STORMS

A geomagnetic storm is a major disturbance of earth's magnetosphere that occurs when there is very efficient exchange of energy from the solar wind into the space environment surrounding the earth. These storms results from variations in the solar wind that produces major changes in the currents, plasmas, and fields in earth's magnetosphere. The solar wind conditions that are effective for creating geomagnetic storms are sustained periods of high-speed solar wind, and most importantly, a southward directed solar wind

magnetic field (opposite to the direction of earth's field) at the dayside of the magnetosphere. This condition is effective for transferring energy from solar wind to the earth's magnetic field.[5] The largest storms that result from these conditions are associated with solar coronal mass ejections (CMEs) where billion tons or so of plasma from the sun, with its embedded magnetic field, arrive at earth. CMEs typically take several days to arrive at earth, but have been observed, for some of the most intense storms, to arrive in as short as eighteen hours. Another solar wind disturbance that creates conditions favourable to geomagnetic storms is a high-speed solar wind stream (HSS). The high-speed solar wind stream overtakes the slow solar wind streams as they propagate outward creating co-rotating interaction regions (CIRs). These regions are often related to geomagnetic storms that while less intense than CME storms, often can deposit more energy in earth's magnetosphere over a long interval.[5]

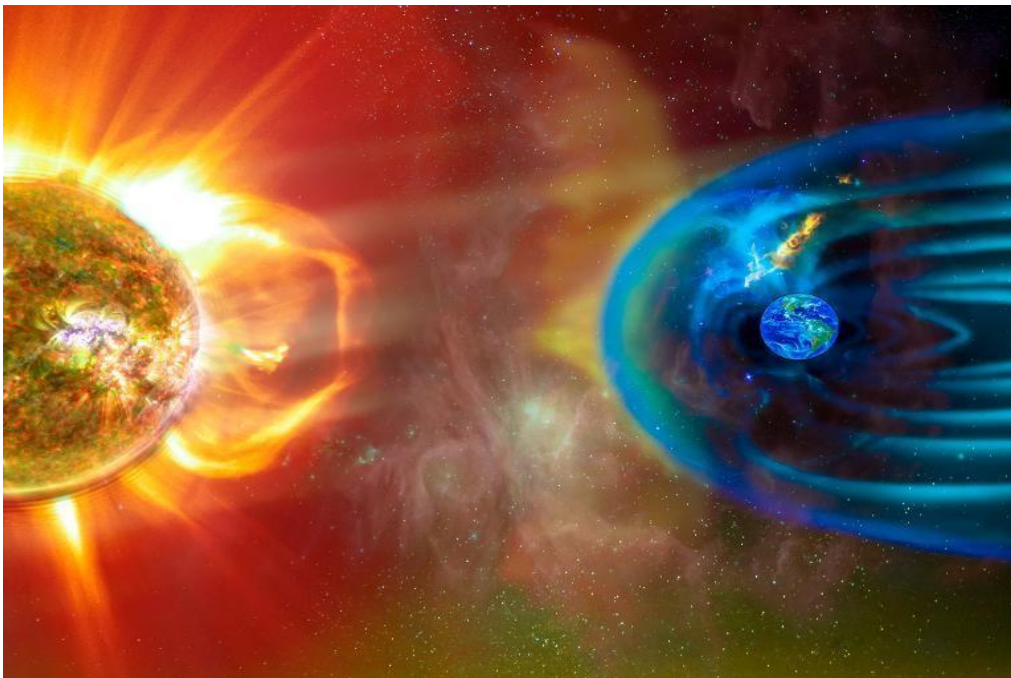


Fig 9: Geomagnetic storms

The frequency of geomagnetic storms increases and decreases with the sunspot cycle. During solar maximum, geomagnetic storms occur more

often, with the majority driven by CMEs. The increase in the solar wind pressure initially compresses the magnetosphere. The solar wind's magnetic field interacts with the earth's magnetic field and transfers an increased energy into the magnetosphere. Both interactions cause an increase in plasma movement through the magnetosphere and an increase in electric current in the magnetosphere and ionosphere. During the main phase of a geomagnetic storm, electric current in the magnetosphere creates a magnetic force that pushes out the boundary between the magnetosphere and the solar wind.[9]

The largest recorded geomagnetic storm, the Carrington event in September 1859, took down parts of the recently created US telegraph network, starting fires and shocking some telegraph operators. In 1989, a geomagnetic storm energized ground induced currents that disrupted electric power distribution throughout most of Quebec and cause aurorae as far south as Texas.[9]

1.6. SUN-EARTH CONNECTIONS

When the solar wind travels with the IMF, the charged particles and magnetic fields interact with the Earth's magnetic field. The Earth's magnetic field, as it stretches out in space, is known as its magnetosphere. The solar wind pushes on the side of the magnetosphere facing the sun, and pulls it out on the side facing away from the sun. The pulling forms a long tail moving away from the sun, and thus the magnetosphere resembles a wind-sock blowing in the wind. Electrical current flows in the magnetosphere, and generates the light in the sky known as the Northern and Southern lights. Together these lights are known as aurora.[11]

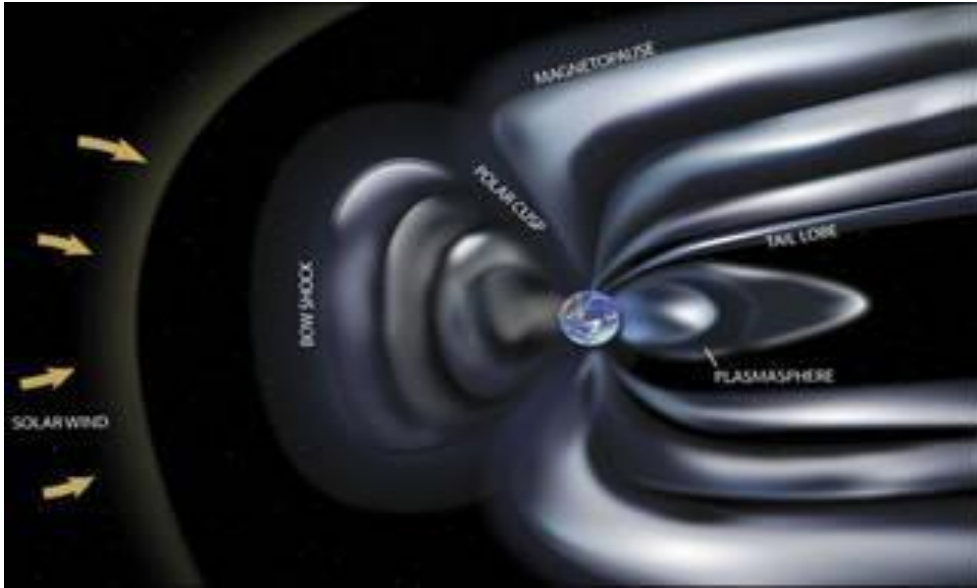


*Fig 10: Earth's magnetosphere as it would look if we had "magnetic field glasses". The shape is created by the interaction of the solar wind with Earth's intrinsic magnetic field.
(Credits: UC Regents)*

The term space weather refers to conditions on the sun and in the solar wind, magnetosphere, ionosphere and thermosphere that can influence the performance and reliability of space-borne and ground-based technological systems and that can affect human life and earth. Our society has become increasingly vulnerable to disturbances in near-earth space weather, in particular to those initiated by explosive events on the sun like solar flares, solar energetic particles (SEPs), and coronal mass ejections (CMEs).[1]

Solar flares release flashes of radiation covering an immense wavelength range (from radio waves to Gamma-rays) that can, heat up the terrestrial atmosphere within minutes such that satellites drop into lower orbits. SEPs accelerated to near-relativistic energies during major solar storms arrive at the Earth's orbit within minutes and may, among other things, severely endanger astronauts travelling through interplanetary space - that is outside the Earth's protective magnetosphere. CMEs ejected into interplanetary space as gigantic clouds of ionized gas, that after a few hours or days may eventually hit the Earth and cause geomagnetic storms.[3]

2. DATA ANALYSIS AND INTERPRETATION

In this project we have analysed the effects of solar wind transients on our Earth. The program codes were written in Root software, which enables statistically sound scientific analysis and visualization of large amount of data. We are analysing the solar wind parameter data such as dynamic pressure, scalar magnetic field, and magnetic field components along with SymH and DST index data for a period from 2001 to 2020 with a four year gap. The one-minute resolution solar wind parameters were obtained from the OMNI Data service (<https://omniweb.gsfc.nasa.gov/>) developed and supported by NASA.

As a first step, we observed the events of flow pressure. We are using the threshold of 3σ level of dynamic pressure and identifying events above this level. Then the corresponding values of B total, V total and the DST values of each year were noted. With the data obtained we plotted graphs and found that they didn't show a good correlation.

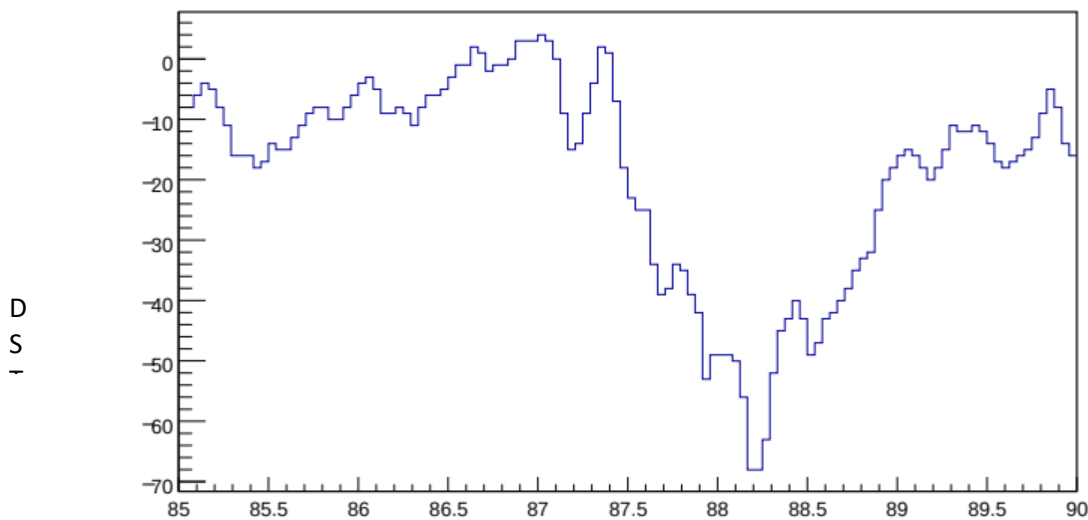


Fig 11. DST index for the days from 85 to 90 of 2012

As a second step, smoothening of flow pressure for each year was done using coded program. Then we integrated the flow pressure, magnetic field and the product of flow pressure and magnetic field. The DST values corresponding to each onset and offset time for all the years were noted. Then graphs were plotted with each integrated values and the corresponding DST values for each year.

2.1. Solar Wind Parameters

1. *Magnetic field*- The magnetic field in the solar wind is relatively weak and is carried along by the solar wind. The rotation of the Sun results in the lines of magnetic flux in the solar wind being drawn into Archimedean spirals. This occurs because the Sun revolves once every ~25.5 days while, it takes solar wind several days to reach 1 AU. Therefore, the Sun revolves through a significant angle during the time it takes the solar wind to reach the Earth. The magnetic field in the solar wind, called the interplanetary magnetic field, or IMF, is attached to the Sun at the point where the solar wind began. Thus, the point on the field line attached to the Sun is turned through an angle of 60° relative to the point on the magnetic field line that is at 1 AU. [12] It gives one minute resolution.
2. *Dynamic pressure*- The dynamic pressure of the solar wind and the interplanetary magnetic field (IMF) are important for the interaction of the solar wind with the earth's magnetosphere, and both of these are generally quite variable. The dynamic pressure of the flowing solar wind is $C\rho V^2$. Here C is a constant, V and ρ are the solar wind velocity and ion number density respectively. [12] It gives one minute resolution.
3. *Disturbance storm time index (DST)*- Disturbance Storm Time index measures the variation of magnetic field associated with

magnetosphere. It is used to analyse the strength and duration of geomagnetic storms. DST is a measure of the decrease in the horizontal component of the Earth's magnetic field near the magnetic equator due to increases in the magnetospheric ring current. Values less than -50 nanotesla indicate high geomagnetic activity. [13] It gives one hour resolution.

4. *SymH*- SymH is the symmetric horizontal component of the magnetic field. The SYM - index represents the global Earth's magnetic field variations. The magnetic observatories to derive this index are located in low latitude and mid-latitude which are far from equator and auroral region to avoid any contamination of auroral and equatorial electrojet currents. The SymH-index gives the magnetic typical signature during geomagnetic storm. For instance, when there is connection between the magnetospheric ring current and Earth's magnetic field during the storm main phase, the SymH variation decrease. While during the magnetospheric compression, the SymH variation increase, the signature of the eastward magnetopause current. The SymH-index pattern also indicates the different phases of geomagnetic storm phases from initial, main and recovery storm phases. [14]

It gives one minute resolution. SymH is essentially the same as the DST index with a different time resolution.

● TProfile

All the histograms used for data analysis were made using TProfile function provided in Root. Profile histograms are used to display the mean value of Y and its error for each bin in X. The displayed error is by default the standard error on the mean (that is, the standard deviation divided by the \sqrt{n}). Profile histograms are elegant replacement of two-dimensional histograms. The inter-relation of two measured

quantities X and Y can always be visualized by a two-dimensional histogram or scatter plot, but if Y is an unknown (but single-valued) approximate function of X, this function is displayed by a profile histogram with much better precision than by a scatter plot.

2.2. Variation of Flow pressure and Magnetic field with DST

We have analysed the solar wind parameter data such as dynamic pressure, scalar magnetic field, and magnetic field components along with the SymH and DST index data for a period from 2001 to 2020. We are using the threshold of 3σ level of dynamic pressure and identifying events above this level.

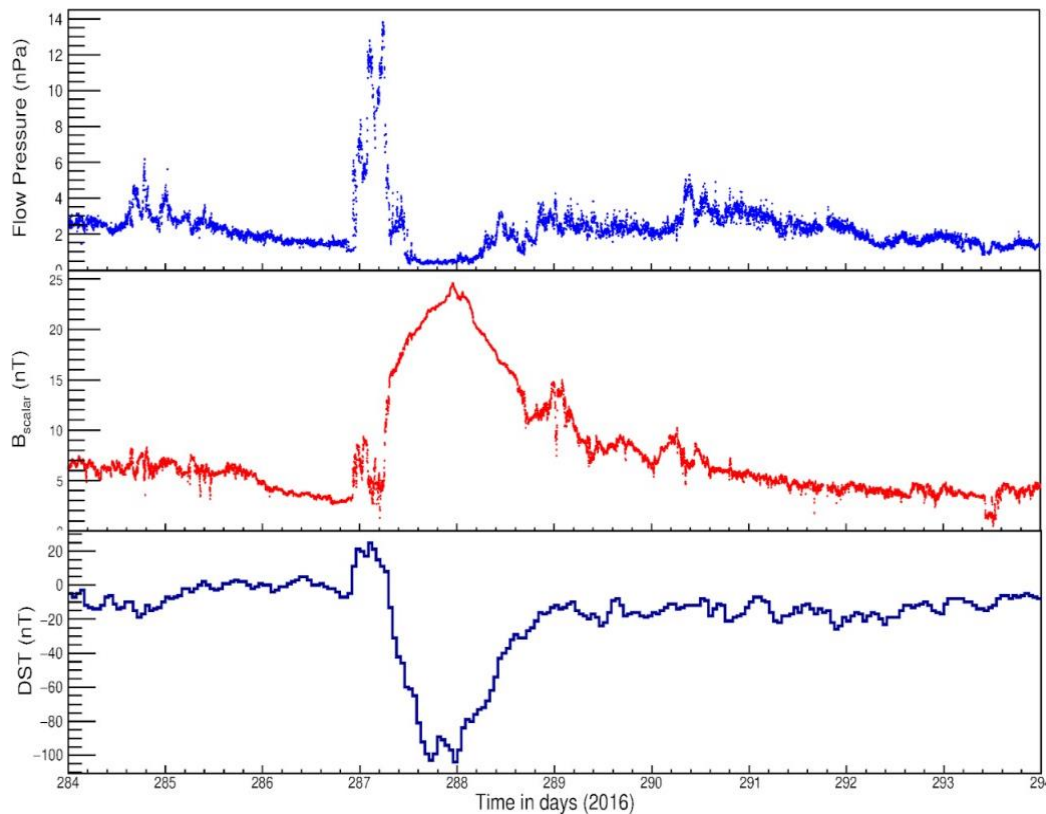


Fig 12: First panel shows the variation of dynamic pressure for the period of 10 days from day number 284 of 2016, second panel shows the variation of scalar magnetic field and the third panel shows the DST index for the same period of time.

In fig 12, the first panel shows the plot of variation of dynamic pressure for the period of ten days from day number 284 of 2016. The time in days is in x-axis and the dynamic pressure is in the y-axis. The second panel indicates the plot of the variation of scalar magnetic field for the same period of time. The time in days is taken along the x-axis and the scalar magnetic field is taken along the y-axis. The third panel shows the DST index for the same period of time. Here DST values are taken along the y-axis and time in days along the x-axis. From the figure we can see an enhancement in flow pressure. With respect to the flow pressure there is an increase in the magnetic field and a decrease in DST. Because of this pressure enhancement, the magnetosphere is compressing and we can see a peak in DST. Then with respect to the increase in magnetic field, the DST is decreasing.

2.3. Dependency of Dynamic pressure and Magnetic field on SymH

We have seen in the fig 12 that, there is an enhancement in the flow pressure and relative to it a change in magnetic field and DST is also observed. So, we are going to analyse the dependency of dynamic pressure and magnetic field on DST. For this, we have analysed all the events from 2001 to 2020 with a four year gap. From them 1650 events were studied to observe their dependency on DST. These events are linked with TProfile. In the case of magnetic field, we use a range of 0 to 40 nT with a bin width of 0.5 nT. Similarly, for dynamic pressure we use a range of 0 to 40 nPa with the same bin width.

Fig 13 indicates the dependency of dynamic pressure on SymH. Dynamic pressure is taken along the x-axis and the SymH is taken along the y-axis. Similarly, fig 14 shows the dependency of scalar magnetic field along the x-axis and SymH along the y-axis. We found a good correlation of SymH

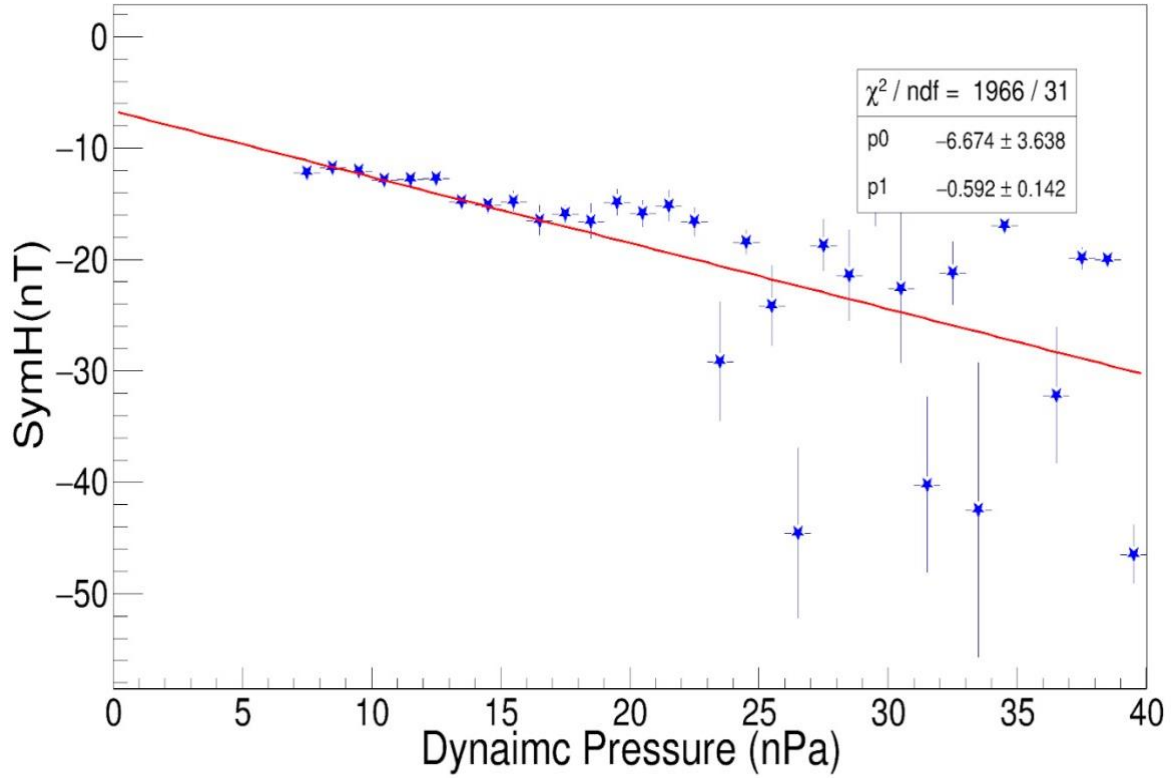


Fig 13: Dependency of dynamic pressure on the SymH

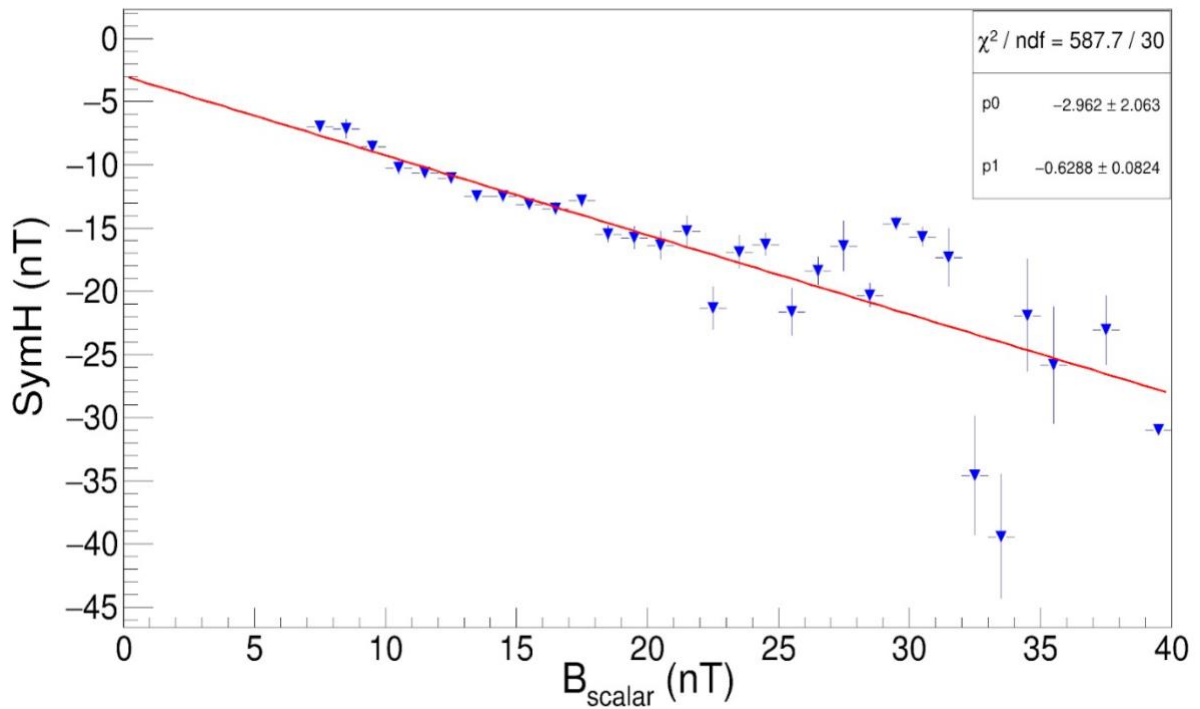


Fig 14: Dependency of scalar magnetic field on SymH

decrease with both magnetic field and dynamic pressure strengths. The dependency of dynamic pressure of SymH is $\sim 0.592 \pm 0.142$ nT/nPa and that of magnetic field on SymH is $\sim 0.6288 \pm 0.0824$.

2.4. Data Analysis by Integration

The integration was done to find the total influence of pressure energy and magnetic energy and also the combined energy with the geomagnetic storm. We have used a threshold of 3σ level of dynamic pressure and magnetic field and the integration was done for events above this level. On integrating, we get a proxy value of pressure and magnetic field which indicates the total dynamic pressure and total magnetic pressure applied on the Earth's magnetosphere.

❖ 2004

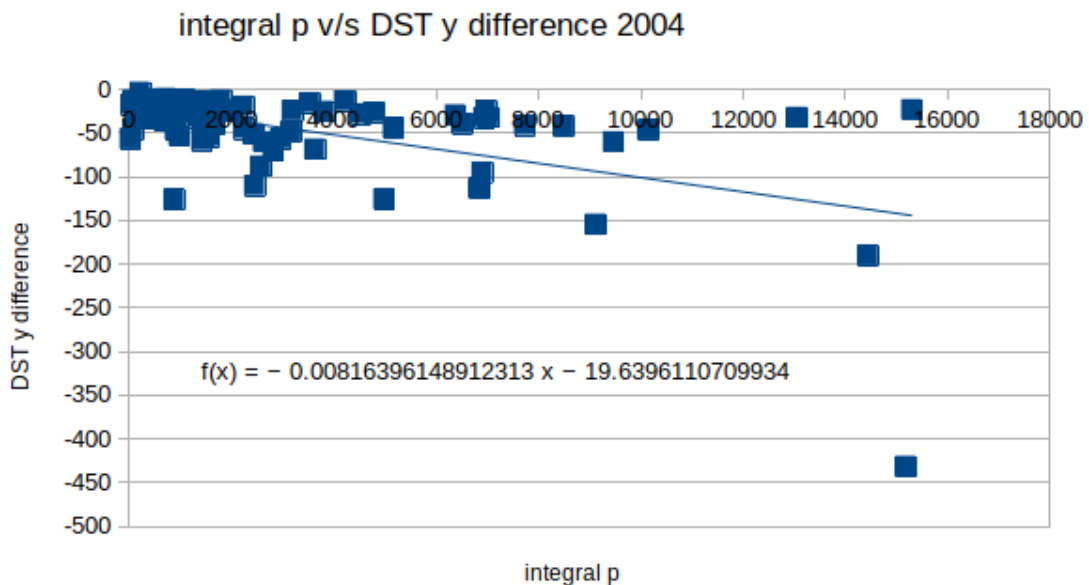


Fig 15: A plot of integrated values of pressure and events in DST profile

The figures 15 and 16 show the plots of integrated values of pressure and magnetic field with the events in DST profile for the year 2004. Each point indicates events. Pressure is measured in nano Pascal, while DST and

magnetic field are measured in nano Tesla. We have obtained a plot with clustered points at the starting and further the values get scattered.

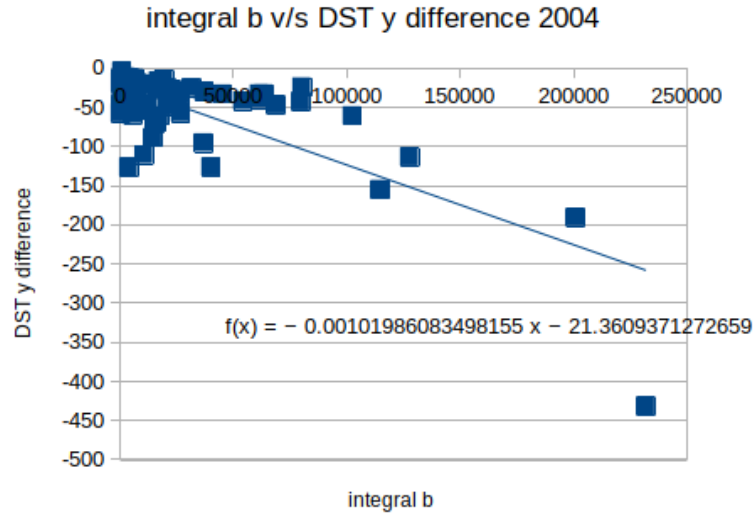


Fig 16: A plot of integrated values of magnetic field and events in DST profile

A trend line was set for each plot showing its equation. Also in each case, the correlation between the corresponding quantities were calculated. In fig 15, the integrated values of pressure are taken along the x-axis and the events in DST profile along the y-axis. The trend line shows an increase and its equation gives a slope of ~ -0.008163 . The correlation is ~ -0.547805 . In fig 16, the integrated values of magnetic field are taken along the x-axis and events in DST profile are taken along the y-axis. The trend line shows an increase with its slope ~ -0.000336 . Its correlation is ~ -0.767304 .

The figures 17 and 18 show the plots of integrated values of pressure and magnetic field with the onset time for the year 2004. Each point indicates events. Pressure is measured in nano Pascal and magnetic field is measured in nano Tesla. We have obtained a plot with clustered points at the starting and further the values get scattered.

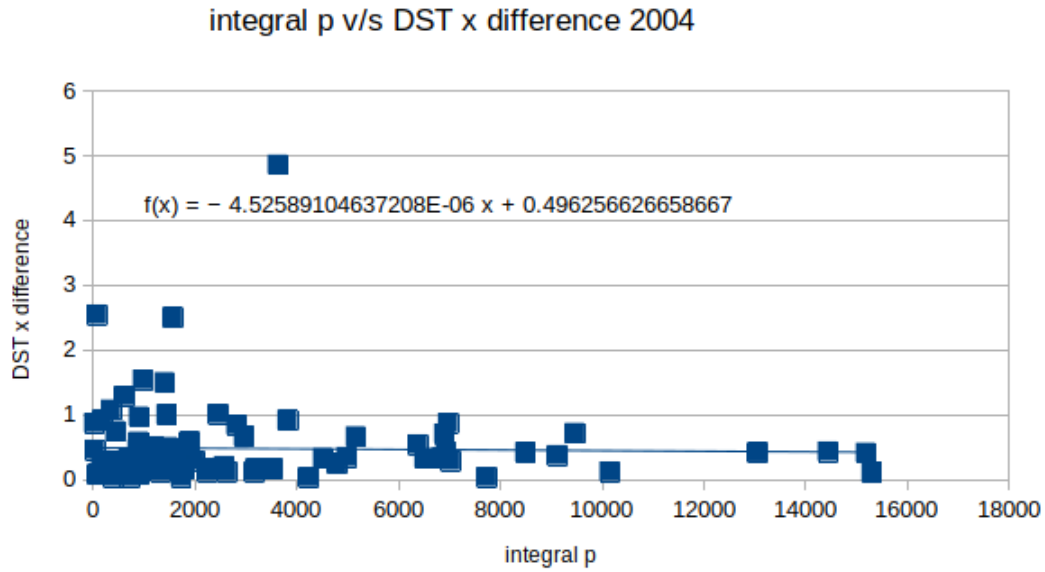


Fig 17: A plot of integrated values of pressure onset time

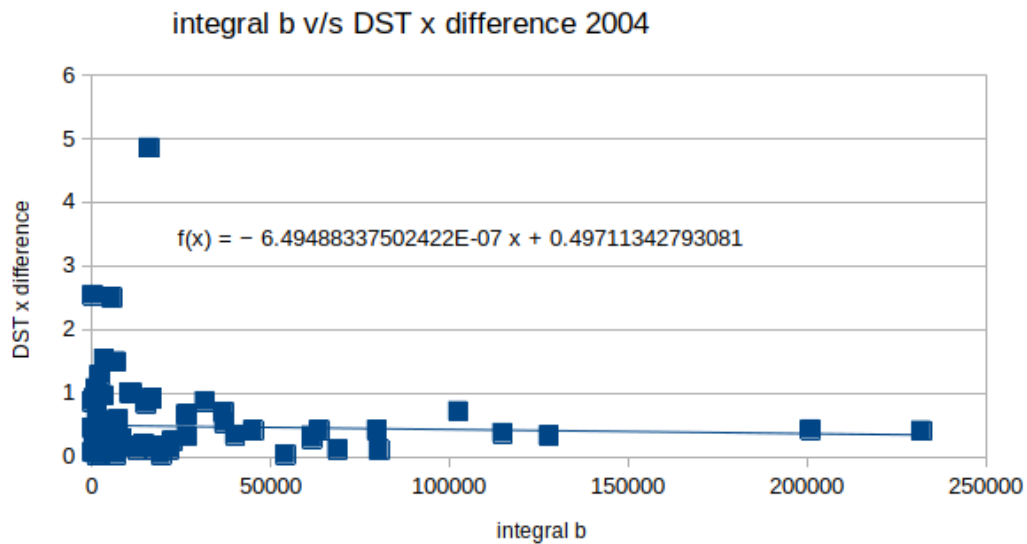


Fig 18: A plot of integrated values of magnetic field and onset time

A trend line was set for each plot showing its equation. Also in each case, the correlation between the corresponding quantities were calculated. In fig 17, the integrated values of pressure are taken along the x-axis and the onset time along the y-axis. The trend line shows an increase and its equation gives a slope of $\sim -4.53E-12$. Its correlation is ~ -0.024465 . In fig 18, the integrated values of magnetic field are taken along the x-axis and the onset time is taken

along the y-axis. The trend line shows a decrease with its slope $\sim -6.49\text{E-}07$. Its correlation is ~ -0.039365 .

❖ 2008

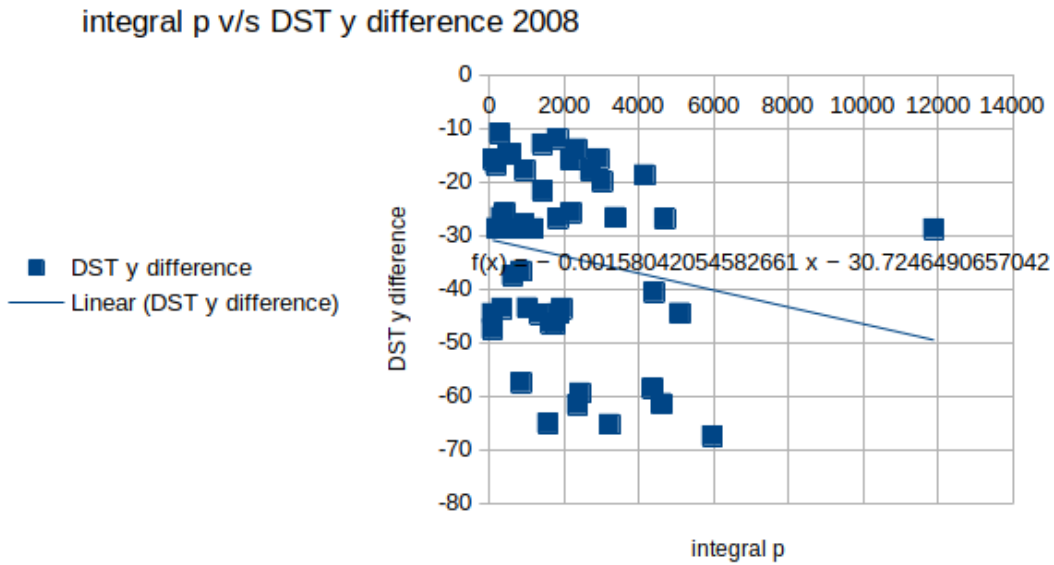


Fig 19: A plot of integrated values of pressure and events in DST profile

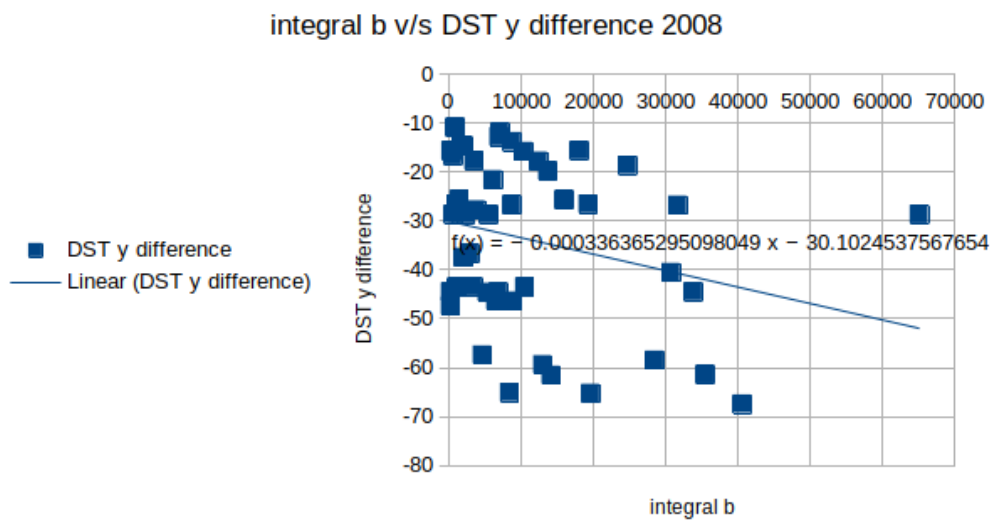


Fig 20: A plot of integrated values of magnetic field and events in DST profile

The figures 19 and 20 show the plots of integrated values of pressure and magnetic field with the events in DST profile for the year 2008. Each point indicates events. Pressure is measured in nano Pascal, while DST and magnetic field are measured in nano Tesla. We have obtained a plot with clustered points at the starting and further the values get scattered. A trend

line was set for each plot showing its equation. Also in each case, the correlation between the corresponding quantities were calculated. In fig 19, the integrated values of pressure are taken along the x-axis and the events in DST profile along the y-axis. The trend line shows an increase and its equation gives a slope of ~ -0.001580 . Its correlation is ~ -0.542476 . In fig 20, the integrated values of magnetic field are taken along the x-axis and events in DST profile are taken along the y-axis. The trend line shows an increase with its slope ~ -0.000336 . Its correlation is ~ -0.545133 .

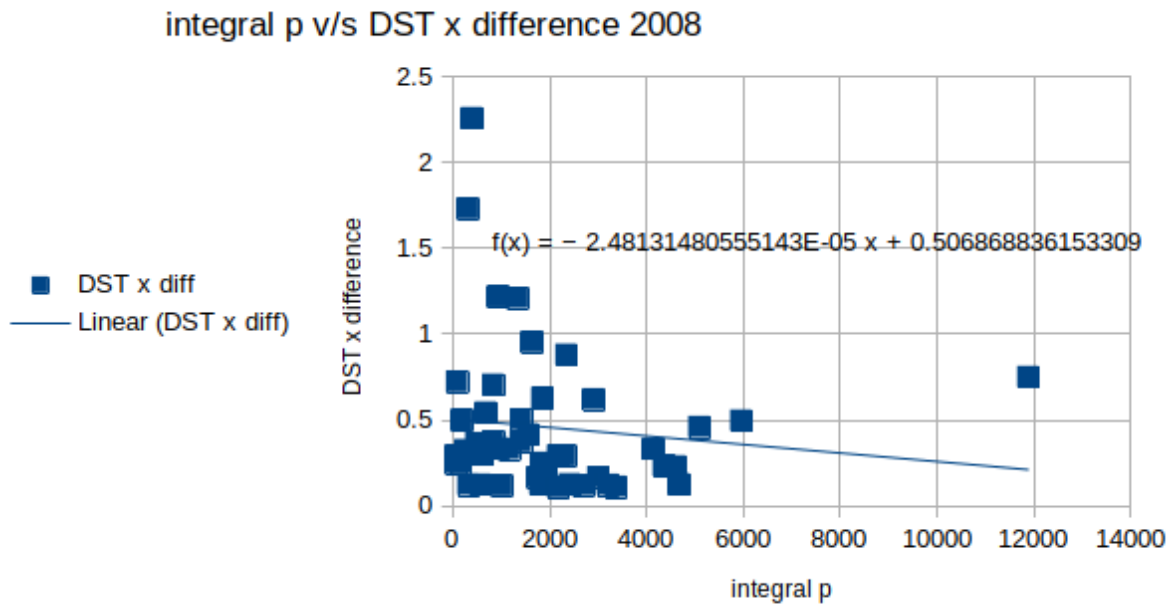


Fig 21: A plot of integrated values of pressure and onset time

The figures 21 and 22 show the plots of integrated values of pressure and magnetic field with the onset time for the year 2008. Each point indicates events. Pressure is measured in nano Pascal and magnetic field is measured in nano Tesla. We have obtained a plot with clustered points at the starting and further the values get scattered. A trend line was set for each plot showing its equation. Also in each case, the correlation between the corresponding quantities were calculated.

integral b v/s DST x difference 2008

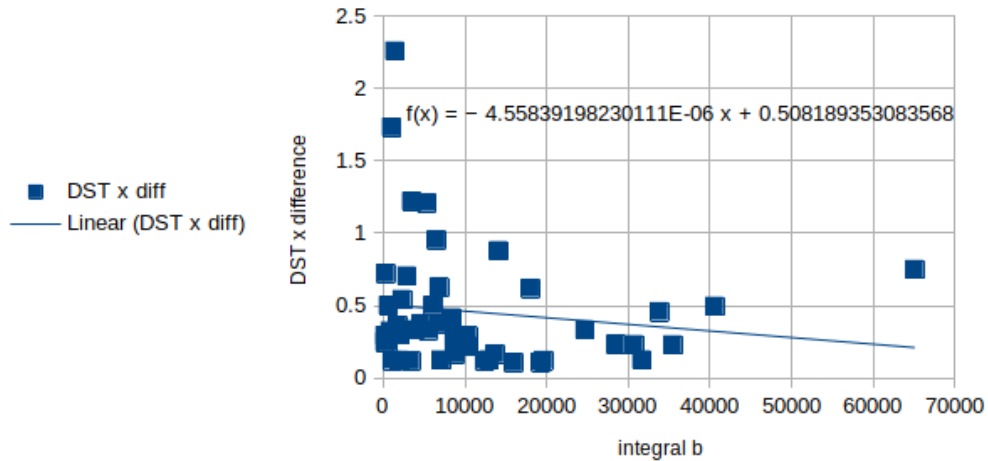


Fig 22: A plot of integrated values of magnetic field and onset time

In fig 21, the integrated values of pressure are taken along the x-axis and the onset time along the y-axis. The trend line shows an increase and its equation gives a slope of $\sim -2.48E-05$. Its correlation is ~ -0.129701 . In fig 22, the integrated values of magnetic field are taken along the x-axis and the onset time is taken along the y-axis. The trend line shows a decrease with its slope $\sim -4.56E-06$ Its correlation is ~ -0.145420 .

❖ 2012

integral p v/s DST y difference 2012

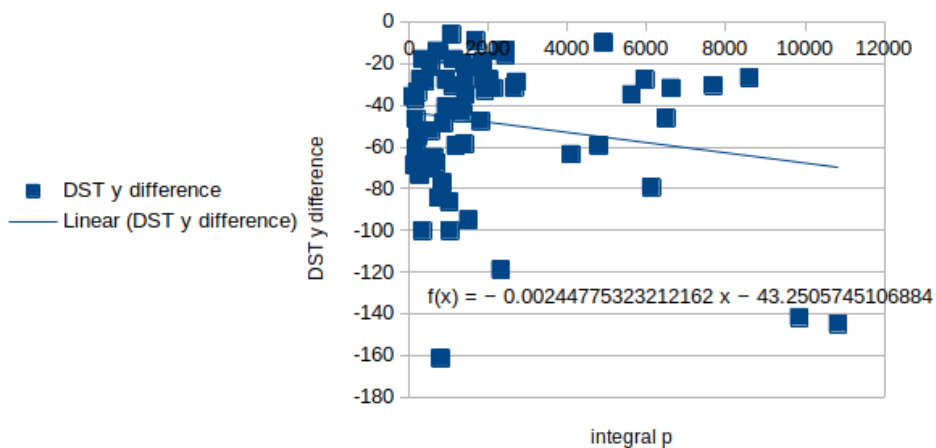


Fig 23: A plot of integrated values of pressure and events in DST profile

integral b v/s DST y difference 2012

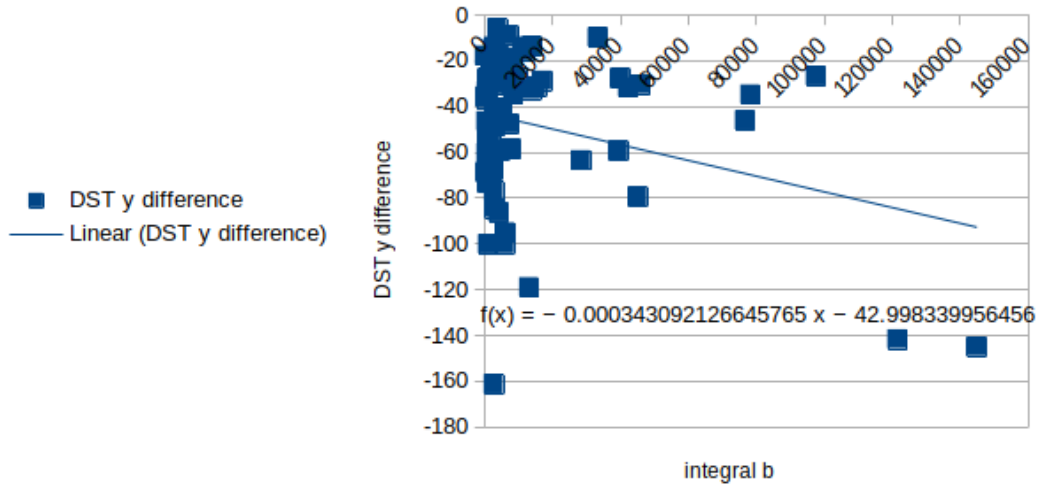


Fig 24: A plot of integrated values of magnetic field and events in DST profile

The figures 23 and 24 show the plots of integrated values of pressure and magnetic field with the events in DST profile for the year 2012. Each point indicates events. Pressure is measured in nano Pascal, while DST and magnetic field are measured in nano Tesla. We have obtained a plot with clustered points at the starting and further the values get scattered. A trend line was set for each plot showing its equation. Also in each case, the correlation between the corresponding quantities were calculated. In fig 23, the integrated values of pressure are taken along the x-axis and the events in DST profile along the y-axis. The trend line shows an increase and its equation gives a slope of ~ -0.007845 . Its correlation is ~ -0.575510 . In fig 24, the integrated values of magnetic field are taken along the x-axis and events in DST profile are taken along the y-axis. The trend line shows an increase with its slope ~ -0.000717 . Its correlation is ~ -0.609618 .

The figures 25 and 26 show the plots of integrated values of pressure and magnetic field with the onset time for the year 2012. Each point indicates events. Pressure is measured in nano Pascal and magnetic field is measured

in nano Tesla. We have obtained a plot with clustered points at the starting and further the values get scattered.

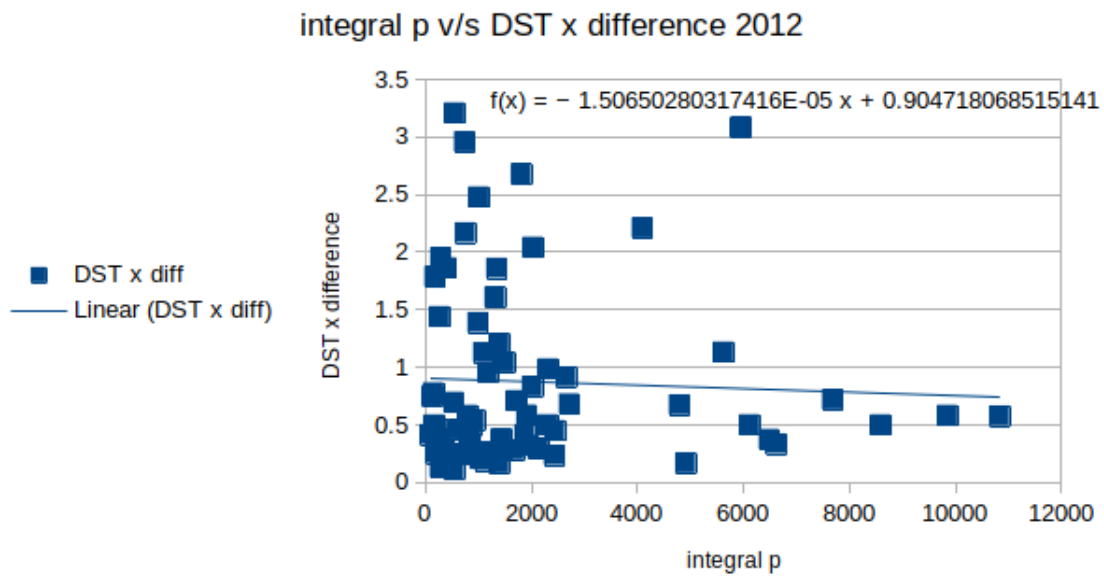


Fig 25: A plot of integrated values of pressure and onset time

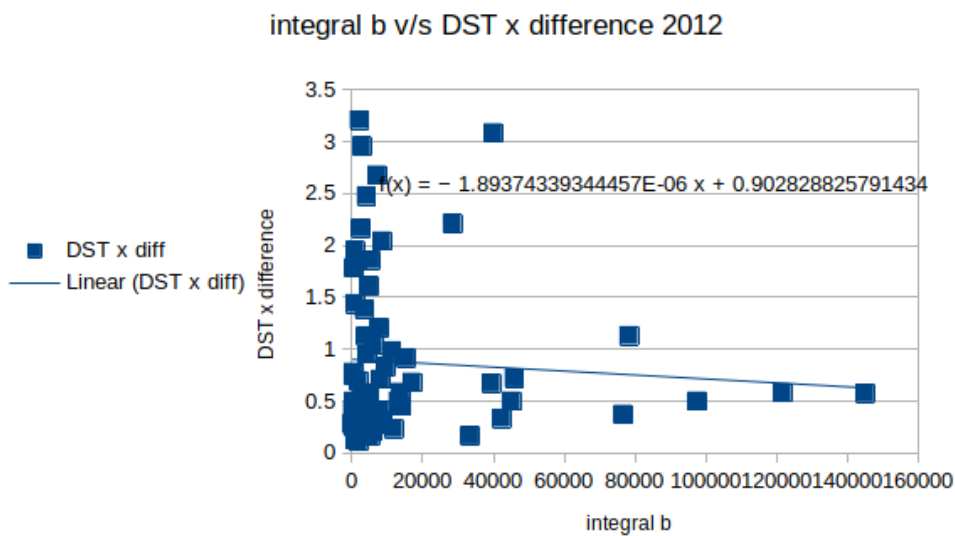


Fig 26: A plot of integrated values of magnetic field and onset time

A trend line was set for each plot showing its equation. Also in each case, the correlation between the corresponding quantities were calculated. In fig 25, the integrated values of pressure are taken along the x-axis and the onset time along the y-axis. The trend line shows a decrease and its equation gives

a slope of $\sim -2.10 \times 10^{-5}$. Its correlation is ~ -0.060442 . In fig 26, the integrated values of magnetic field are taken along the x-axis and the onset time is taken along the y-axis. The trend line shows a decrease with its slope $\sim -2.30 \times 10^{-6}$. Its correlation is ~ -0.076484 .

❖ 2016

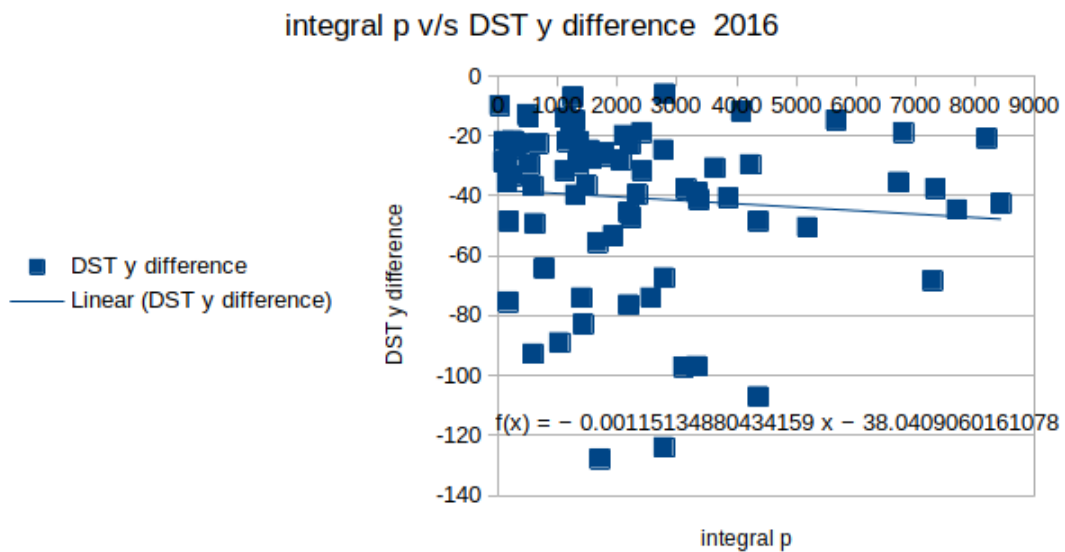


Fig 27: A plot of integrated values of pressure and events in DST profile

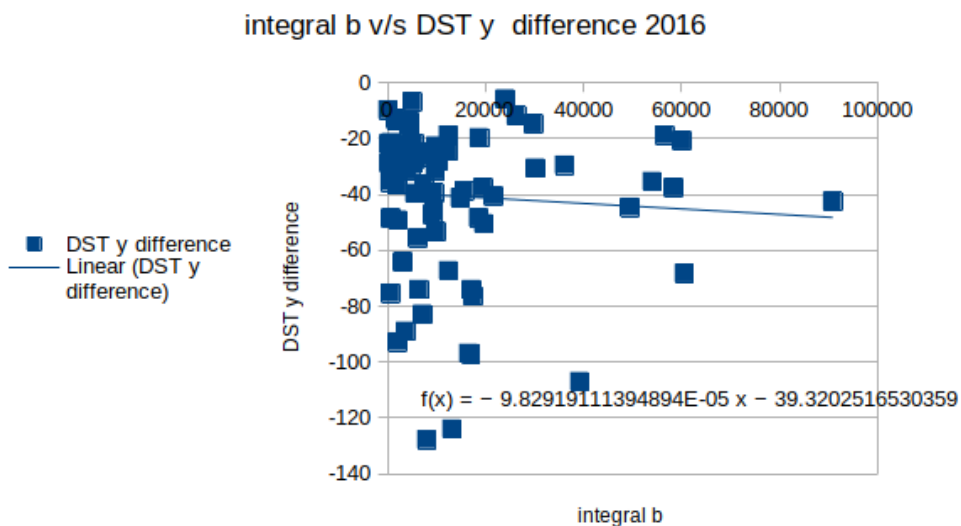


Fig 28: A plot of integrated values of magnetic field and events in DST profile

The figures 27 and 28 show the plots of integrated values of pressure and magnetic field with the events in DST profile for the year 2016. Each point indicates events. Pressure is measured in nano Pascal, while DST and magnetic field are measured in nano Tesla. We have obtained a plot with clustered points at the starting and further the values get scattered. A trend line was set for each plot showing its equation. Also in each case, the correlation between the corresponding quantities were calculated. In fig 27, the integrated values of pressure are taken along the x-axis and the events in DST profile along the y-axis. The trend line shows an increase and its equation gives a slope of ~ -0.006992 . Its correlation is ~ -0.462505 . In fig 28, the integrated values of magnetic field are taken along the x-axis and events in DST profile are taken along the y-axis. The trend line shows an increase with its slope ~ -0.000799 . Its correlation is ~ -0.522577 .

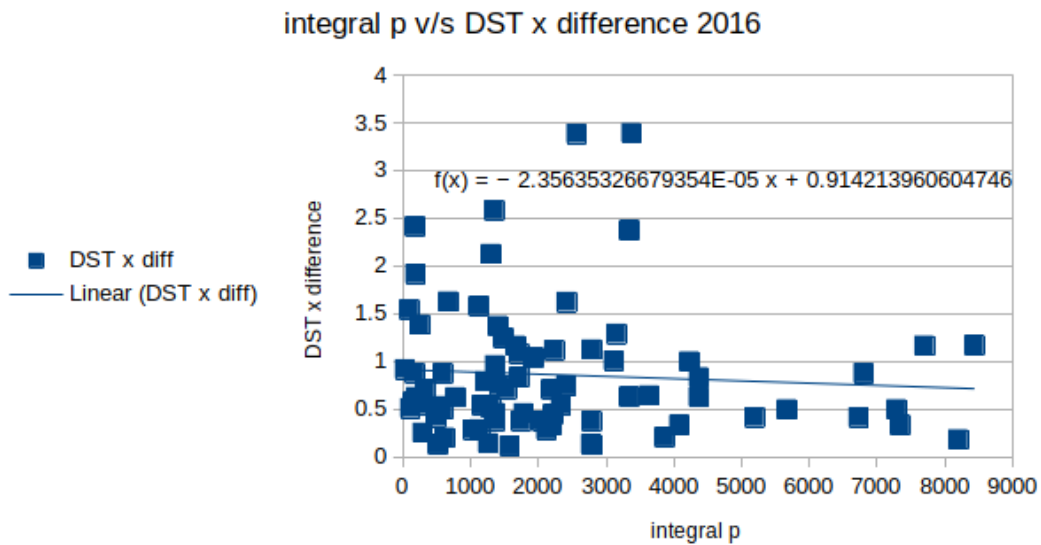


Fig 29: A plot of integrated values of pressure and onset time

The figures 29 and 30 show the plots of integrated values of pressure and magnetic field with the onset time for the year 2016. Each point indicates events. Pressure is measured in nano Pascal and magnetic field is measured in nano Tesla. We have obtained a plot with clustered points at the starting and further the values get scattered.

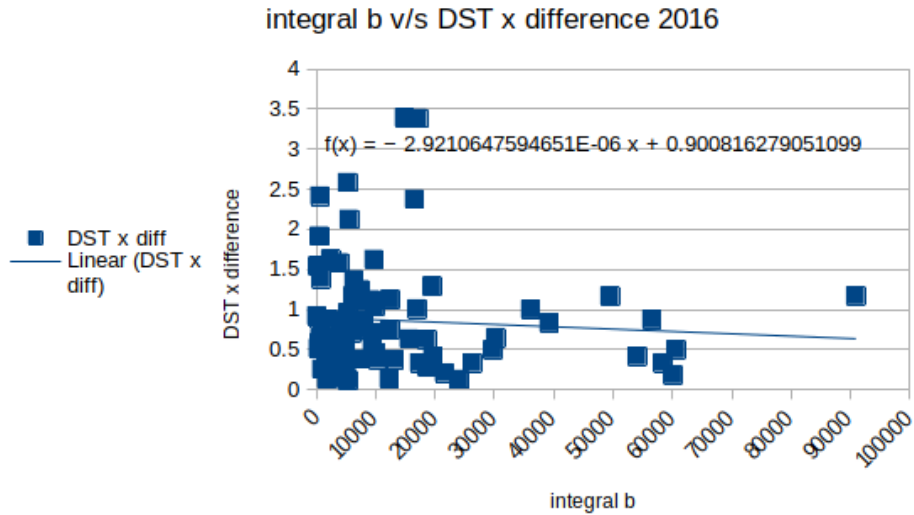


Fig 30: A plot of integrated values of magnetic field and onset time

A trend line was set for each plot showing its equation. Also in each case, the correlation between the corresponding quantities were calculated. In fig 29, the integrated values of pressure are taken along the x-axis and the onset time along the y-axis. The trend line shows an increase and its equation gives a slope of $\sim -3.03E-05$. Its correlation is ~ -0.077141 . In fig 30, the integrated values of magnetic field are taken along the x-axis and the onset time is taken along the y-axis. The trend line shows an increase with its slope $\sim -3.96E-06$. Its correlation is ~ -0.084474 .

❖ 2020

The figures 31 and 32 show the plots of integrated values of pressure and magnetic field with the events in DST profile for the year 2020. Each point indicates events. Pressure is measured in nano Pascal, while DST and magnetic field are measured in nano Tesla. We have obtained a plot with clustered points at the starting and further the values get scattered. A trend line was set for each plot showing its equation. Also in each case, the correlation between the corresponding quantities were calculated.

integral p v/s DST y difference 2020

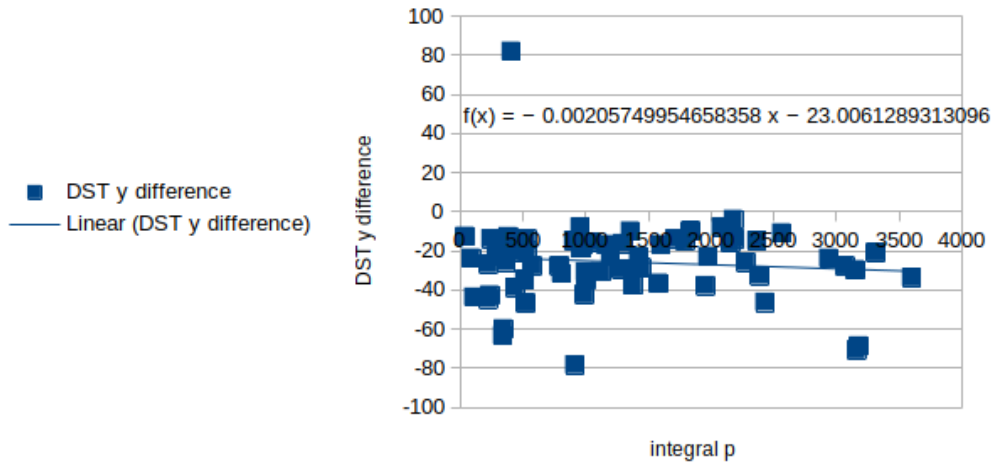


Fig 31: A plot of integrated values of pressure and events in DST profile

integral b v/s DST y difference 2020

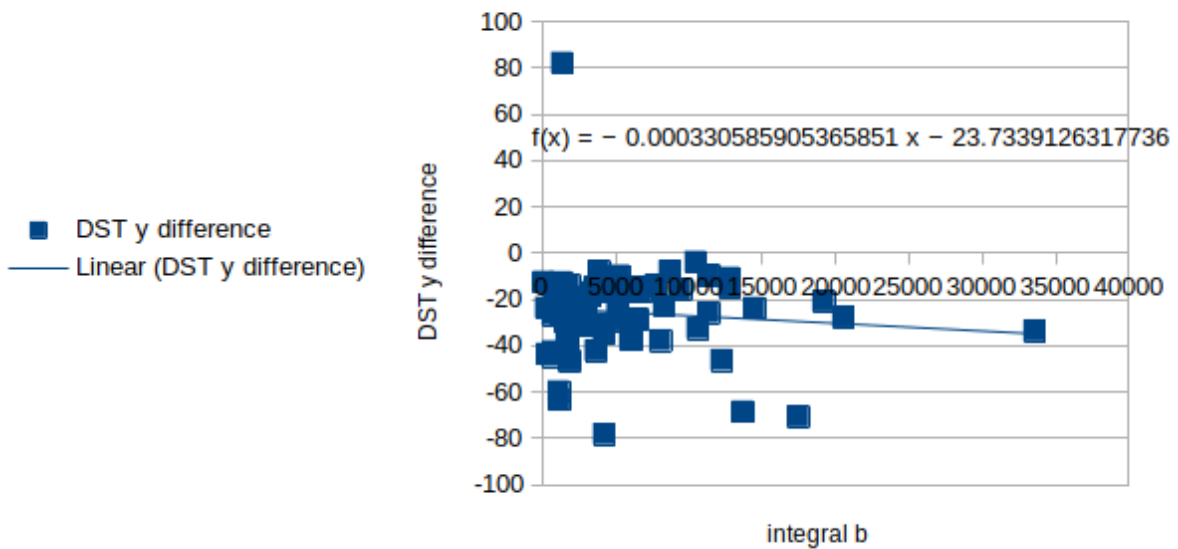


Fig 32: A plot of integrated values of magnetic field and events in DST profile

In fig 31, the integrated values of pressure are taken along the x-axis and the events in DST profile along the y-axis. The trend line shows an increase and its equation gives a slope of ~ -0.004500 . Its correlation is ~ -0.207191 . In fig 32, the integrated values of magnetic field are taken along the x-axis and events in DST profile are taken along the y-axis. The trend line shows an increase with its slope ~ -0.000755 . Its correlation is ~ -0.217067 .

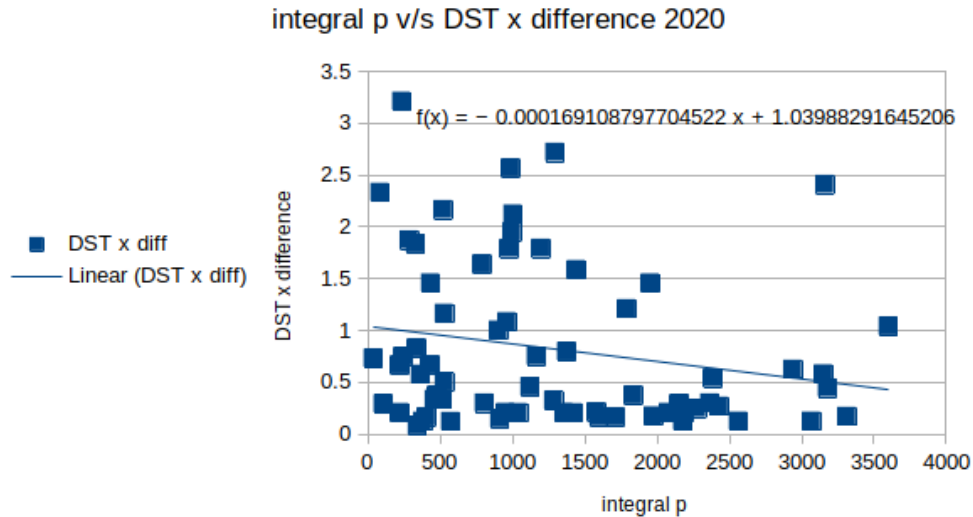


Fig 33: A plot of integrated values of pressure and onset time

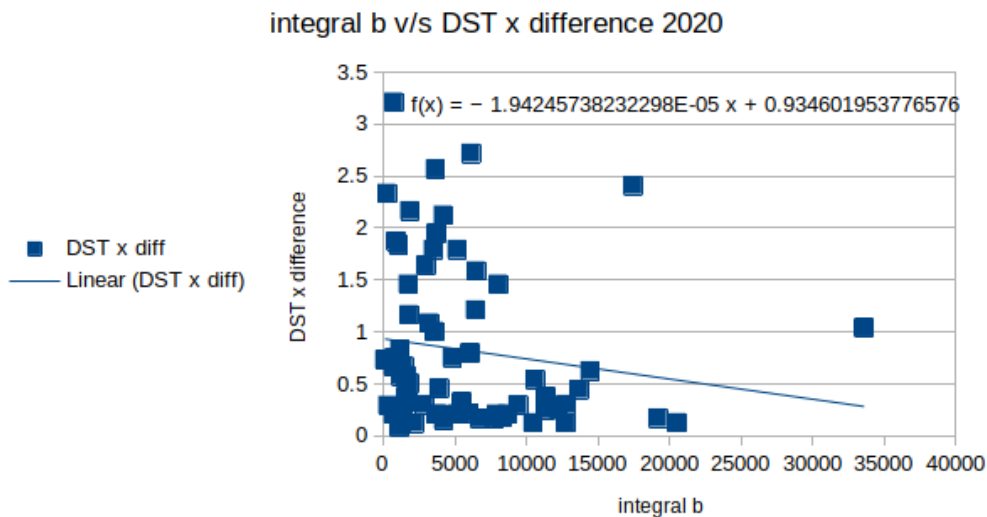


Fig 34: A plot of integrated values of magnetic field and onset time

The figures 33 and 34 show the plots of integrated values of pressure and magnetic field with the onset time for the year 2020. Each point indicates events. Pressure is measured in nano Pascal and magnetic field is measured in nano Tesla. We have obtained a plot with clustered points at the starting and further the values get scattered. A trend line was set for each plot showing its equation. Also in each case, the correlation between the corresponding quantities were calculated. In fig 33, the integrated values of pressure are taken along the x-axis and the onset time along the y-axis. The trend line shows an increase and its equation gives a slope of ~ -0.0001709

Its correlation is ~ -0.190319 . In fig 34, the integrated values of magnetic field are taken along the x-axis and the onset time is taken along the y-axis. The trend line shows an increase with its slope $\sim -1.93E-05$. Its correlation is ~ -0.1341628 .

2.5. Observations

1. Table 1:- DST

YEAR	SLOPE		CORRELATION	
	<i>Integral p with DST</i>	<i>Integral b with DST</i>	<i>Integral p with DST</i>	<i>Integral b with DST</i>
2004	-0.00816396	-0.00101986	-0.54780599	-0.76730481
2008	-0.00158042	-0.00033636	-0.54247695	-0.54513386
2012	-0.00784554	-0.00071719	-0.57551071	-0.6096185
2016	-0.00699241	-0.00079957	-0.46250564	-0.52257767
2020	-0.00450089	-0.00075541	-0.207191001	-0.21706749

2. Table 2:- ONSET TIME

YEAR	SLOPE		CORRELATION	
	<i>Integral p with onset time</i>	<i>Integral b with onset time</i>	<i>Integral p with onset time</i>	<i>Integral b with onset time</i>
2004	-4.53E-12	-6.49E-07	-0.024462525	-0.03936571
2008	-2.48E-05	-4.56E-06	-0.12970148	-0.14542044
2012	-2.10E-05	-2.30E-06	-0.06044257	-0.07648459
2016	-3.03E-05	-3.96E-06	-0.07714143	-0.08447456
2020	-0.00017098	-1.93E-05	-0.19031971	-0.13416284

Table 1 shows the slope and correlation of the pressure and magnetic field with the events in the DST profile for five years 2004, 2008, 2012, 2016 and 2020. Table 2 shows the slope and correlation of pressure and magnetic field with the onset time for the same years.

3. CONCLUSION

We have analysed the dependency of dynamic pressure and magnetic field with DST and onset values. Here, we have considered the events of five years and combining the results, we obtained the following plots. Then a straight line is fitted which is shown in red in the plots and in each case the slope and correlation are calculated.

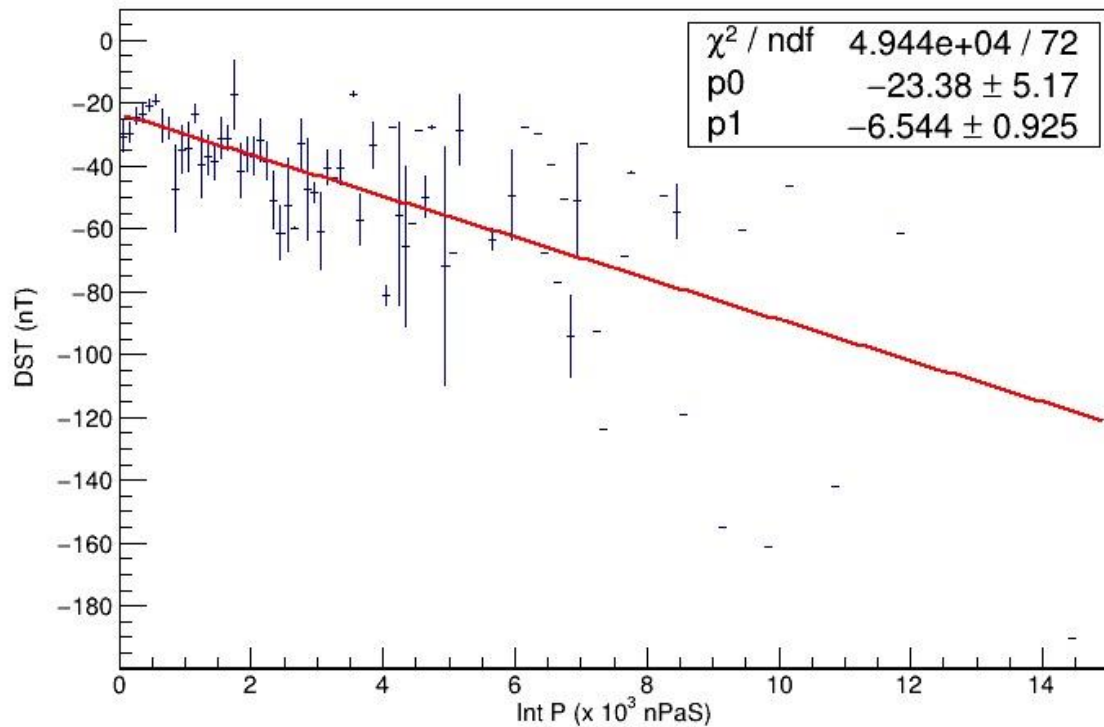


Fig 35: Dependency of dynamic pressure on DST

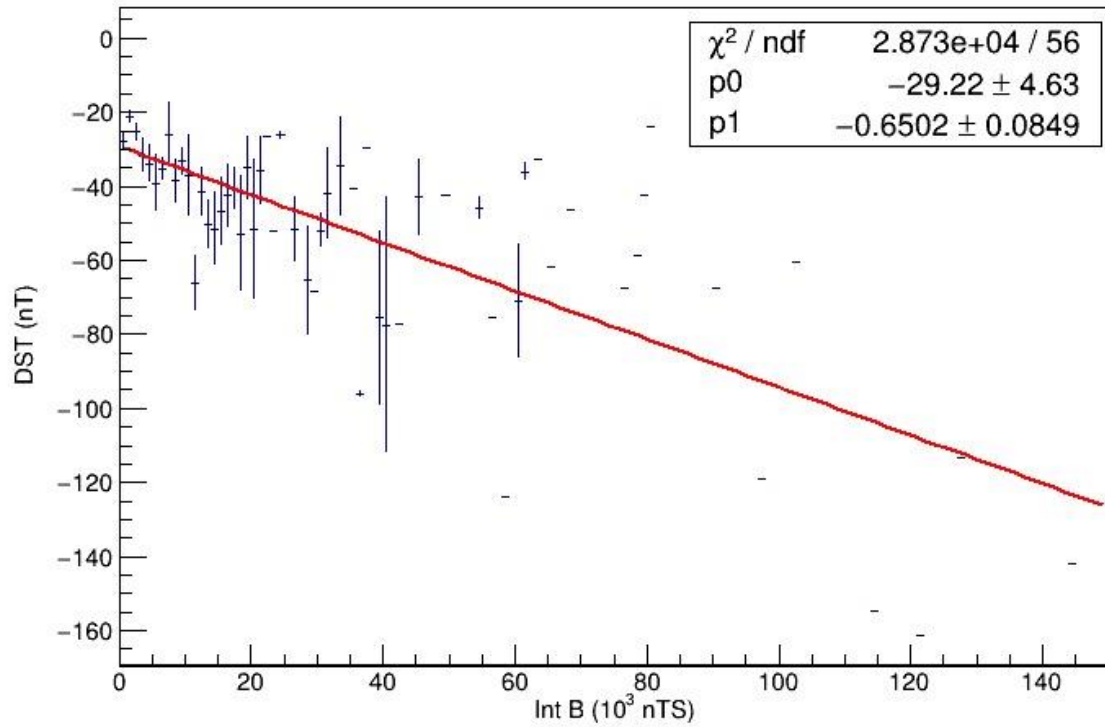


Fig 36: Dependency of magnetic field on DST

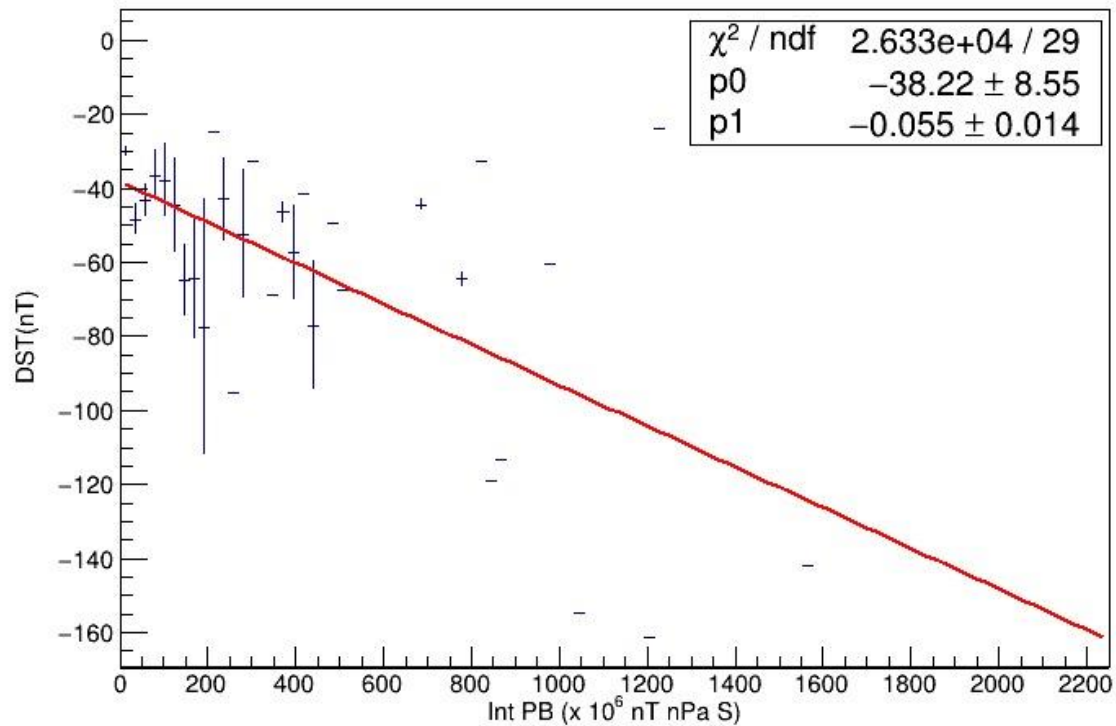


Fig 37: Dependency of $B \cdot P$ on DST

The fig 35 indicates the dependency of dynamic pressure on DST. Dynamic pressure is taken along the x-axis and DST along the y-axis. We have fitted

a straight line and found that it shows a good correlation of DST increase with dynamic pressure with a slope $\sim -6.544 \pm 0.925$. The fig 36 shows the dependency of magnetic field on DST. Magnetic field is taken along the x-axis and DST along the y-axis. On fitting a straight line, we found a good correlation of DST increase with magnetic field with a slope of $\sim -0.6502 \pm 0.0849$. Similarly, the fig 37 indicates the dependency of B*P on DST. B*P is taken along the x-axis and DST along the y-axis. Fitting of a straight line shows a good correlation of DST increase with B*P with a slope of $\sim -0.055 \pm 0.014$.

The fig 38 indicates the dependency of dynamic pressure on onset values. Dynamic pressure is taken along the x-axis and onset along the y-axis. We have fitted a straight line and found that the onset doesn't show a good correlation with dynamic pressure and its slope is $\sim -0.02676 \pm 0.01386$.

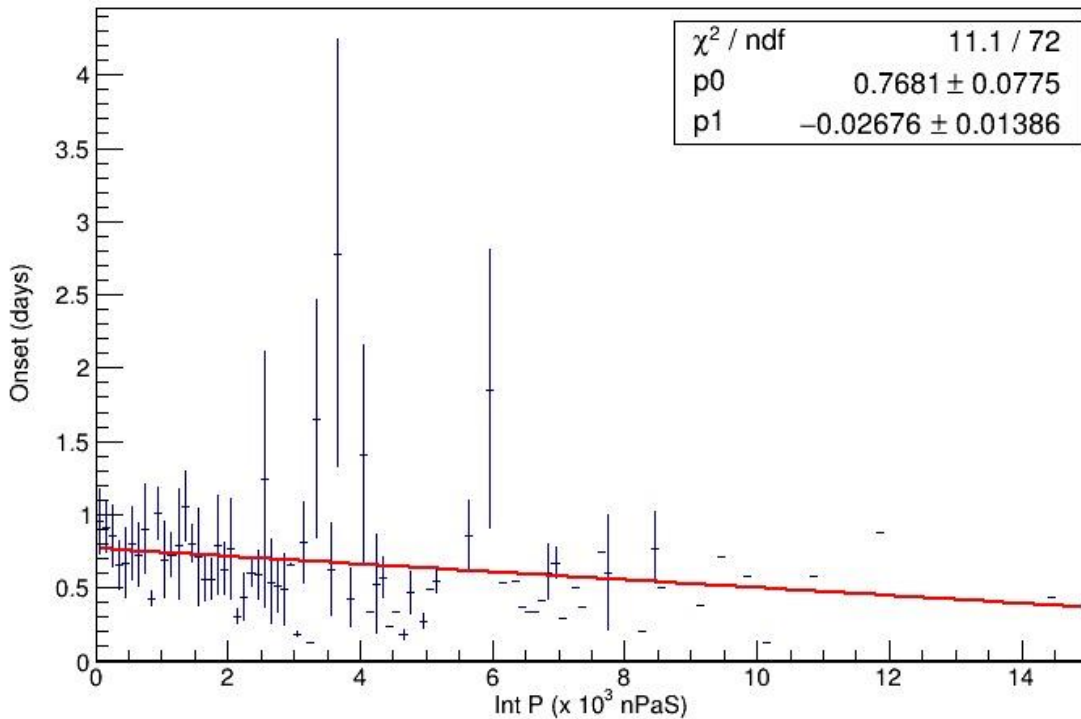


Fig 38: Dependency of dynamic pressure on onset

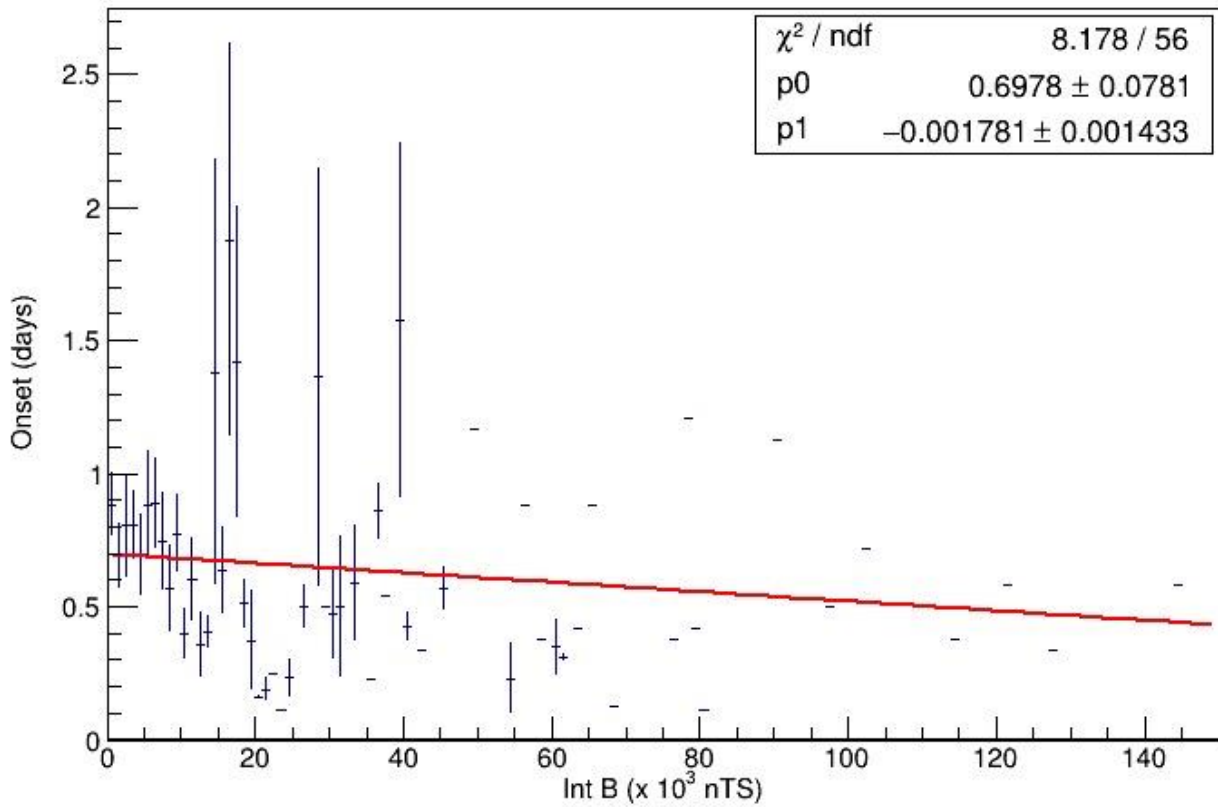


Fig 39: Dependency of magnetic field on onset

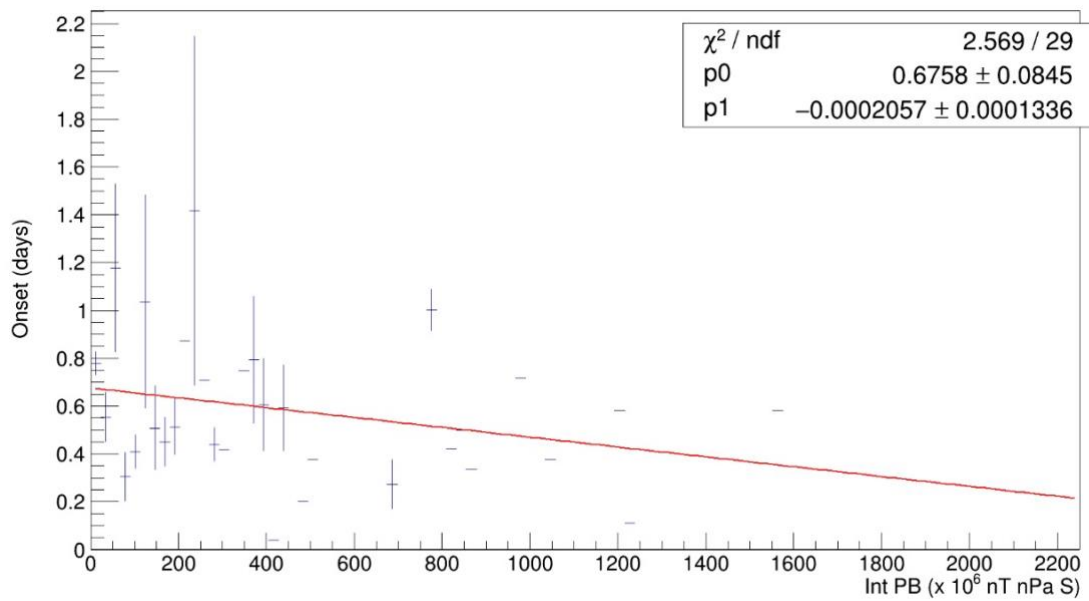


Fig 40: Dependency of B*P on onset

The fig 39 shows the dependency of magnetic field on onset along the y-axis. On fitting a straight line, we can see that it doesn't show a good

correlation with magnetic field and its slope is $\sim -0.001781 \pm 0.001433$. Similarly, the fig 40 indicates the dependency of B*P on onset values. B*P is taken along the x-axis and onset along the y-axis. Fitting of a straight line shows that the onset values doesn't show a good correlation with B*P and its slope is $\sim -0.0002057 \pm 0.0001336$.

From the above results, we can see a good correlation of DST with solar wind parameters that are considered here. A good correlation indicates the major contribution of these parameters on the Earth's magnetosphere. On the other hand, the onset values don't show a good correlation with these parameters. The onset time decreases with strength of the magnetic field.

4. FUTURE WORKS

Due to lack of time, we had to stop our work in between and based on our analysis, we have arrived up to the above conclusions. Here, only dynamic pressure and magnetic field are considered. We plan to expand our work in a more detailed way by considering the other parameters of solar wind. All the results until now are made irrespective of the Bz component of the magnetic field. In further study we will include them.

5. BIBLIOGRAPHY

REFERENCES:

1. KP Arun babu et al. Astronomy and Astrophysics, Babu, A.V. (2014). Coronal Mass Ejections from the Sun - Propagation and Near-Earth Effects. arXiv: Solar and Stellar Astrophysics.
2. <https://www.swpc.noaa.gov/phenomena/coronal-mass-ejections>
3. Schwenn R. Space Weather: The Solar Perspective. Living Rev. Sol. Phys. 3, 2 (2006)
4. <https://scied.ucar.edu/learning-zone/sun-space-weather/solar-corona>
5. <https://www.swpc.noaa.gov/phenomena/geomagnetic-storms>
6. <https://spaceplace.nasa.gov/solar-cycles/en/>
7. <https://www.coursehero.com/study-guides/astronomy/the-structure-andcomposition-of-the-sun/>
8. <https://www.britannica.com/science/solar-cycle>
9. https://en.wikipedia.org/wiki/Geomagnetic_storm
10. N. Gopal Swamy, NASA Goddard Space Flight Centre Greenbelt, MD 20771, USA
11. http://cse.ssl.berkeley.edu/exploringmagnetism/space_weather/presentation.html
12. <https://www.sciencedirect.com/topics/earth-and-planetary-sciences/solarmagnetic-field>
13. <https://www.aer.com/science-research/space/space-weather/spaceweather-index/>
14. Mohd Kasran, Farah & Huzaimy, Jusoh & Enche Ab Rahim, Siti Amalina & Abdullah, Noradlina (2018). Geomagnetically Induced Currents (GICs) in Equatorial Region. 112-117. 10.1109/ICSEngT.2018.8606391.